CARDIFF UNIVERSITY
PRIFYSGOL CAERDYDD

ORCA – Online Research @ Cardiff

This is an Open Access document downloaded from ORCA, Cardiff University's institutional repository:https://orca.cardiff.ac.uk/id/eprint/114477/

This is the author's version of a work that was submitted to / accepted for publication.

Citation for final published version:

Moshkelgosha, Sajad, Masetti, Giulia, Berchner-Pfannschmidt, Utta, Verhasselt, Hedda Luise, Horstmann, Mareike, Diaz-Cano, Salvador, Noble, Alistair, Edelman, Barbel, Covelli, Danila, Plummer, Sue, Marchesi, Julian R. , Ludgate, Marian, Biscarini, Filippo , Eckstein, Anja and Banga, J. Paul 2018. Gut microbiome in BALB/c and C57BL/6J mice undergoing experimental thyroid autoimmunity associate with differences in immunological responses and thyroid function. Hormone and Metabolic Research 50 (12) , pp. 932-941. 10.1055/a-0653-3766

Publishers page: http://dx.doi.org/10.1055/a-0653-3766

Please note:
Changes made as a result of publishing processes such as copy-editing, formatting and page numbers may not be reflected in this version. For the definitive version of this publication, please refer to the published source. You are advised to consult the publisher's version if you wish to cite this paper.

This version is being made available in accordance with publisher policies. See http://orca.cf.ac.uk/policies.html for usage policies. Copyright and moral rights for publications made available in ORCA are retained by the copyright holders.

Gut microbiota in experimental murine model of Graves' orbitopathy established in different environments may modulate clinical presentation of disease.

Giulia Masetti*[1,2], Sajad Moshkelgosha*[3,4,5], Hedda-Luise Köhling[6,7], Danila Covelli[6,8], Jasvinder Paul Banga[3,4], Utta Berchner-Pfannschmidt[3], Mareike Horstmann[3], Salvador Diaz-Cano[9], Gina-Eva Goertz[3], Sue Plummer[6], Anja Eckstein[3], Marian Ludgate[1], ^Filippo Biscarini[1,2,10], ^Julian Marchesi[11,12] and the INDIGO consortium[13].

*these authors contributed equally to the study, ˆ these authors are joint senior author

Institutional addresses of all authors:

1. Division of Infection & Immunity, School of Medicine, Cardiff University, Cardiff, United Kingdom (GM, ML, LZ, FB)
2. Departments of Bioinformatics, PTP Science Park Srl., via Einstein loc. Cascina Codazza, Lodi 29600, Italy (GM, FB)
3. Molecular Ophthalmology (UBP, SM, GEG, MH, AE, JPB), Department of Ophthalmology; University Hospital Essen/University of Duisburg-Essen, 45147 Essen, Germany
4. Faculty of Life Sciences and Medicine (SM, JPB), King's College London, London, SE5 9NU United Kingdom;
5. Latner Thoracic Surgery Laboratories, Toronto General Research Institute, University Health Network and University of Toronto, Toronto, M5G 1L7, Canada (SM)
6. Cultech Ltd., Baglan, Port Talbot, SA127BZ, United Kingdom (SPl, DM, IG)
7. University Hospital Essen, University of Duisburg-Essen, Institute of Medical Microbiology, 45147, Essen, Germany (HLK)
8. Graves' Orbitopathy Center, Endocrinology, Department of Clinical Sciences and Community Health, Fondazione Ca'Granda IRCCS, University of Milan, via Sforza 35, 20122 Milan, Italy (DC, MS, GC)
9. King's College Hospital NHS Foundation Trust (SDC), London, SE5 9RS United Kingdom
10. Italian National Council for Research (CNR), via Bassini 15, 20133 Milan, Italy (FB)
11. School of Biosciences, Cardiff University, Cardiff, United Kingdom (JRM)
12. Center for Digestive and Gut Health, Imperial College London, London, W2 1NY (JRM)
13. INDIGO Consortium, http://www.indigo-iapp.eu

Corresponding author:
Prof. Julian Marchesi
School of Bioscience, Cardiff University
Sir Martin Evans Building, Museum Avenue, Cardiff, CF10 3AX
+44 (0)29 2087 4188
MarchesiJR@cardiff.ac.uk

Abstract

Background: Variation in induced models of autoimmunity has been attributed to the housing environment and its effect on the gut microbiota. In Graves' disease (GD), autoantibodies to the thyrotropin receptor (TSHR) cause autoimmune hyperthyroidism. Many GD patients develop Graves' orbitopathy (GO) characterized by orbital tissue remodeling including adipogenesis. Murine models of GD/GO would help delineate pathogenetic mechanisms and although several have been reported most lack reproducibility. A model comprising immunization of female BALBc mice with a TSHR expression plasmid using *in vivo* electroporation, was reproduced in two independent laboratories. Similar orbital disease was induced in both centers, but differences were apparent (e.g. hyperthyroidism in Center 1 but not Center 2). We hypothesized a role for the gut microbiota influencing the outcome and reproducibility of induced GO.

Results: We combined metataxonomics (16S rRNA gene sequencing) and traditional microbial culture of the intestinal contents from the GO murine model, to analyze the gut microbiota in the two centers. We observed significant differences in alpha, beta-diversity and in the taxonomic profiles, e.g. Operational Taxonomic Units (OTUs) from the genus *Lactobacillus* were more abundant in Center 2, *Bacteroides* and *Bifidobacterium* counts were more abundant in Center 1 where we also observed a negative correlation between the OTUs of the genus *Intestinimonas* and TSHR autoantibodies. Traditional microbiology largely confirmed the metataxonomics data and indicated significantly higher yeast counts in Center 1 TSHR-immunized mice. We also compared the gut microbiota between immunization groups within the Center 2, comprising the TSHR or βgal control immunized mice and naïve untreated mice. We observed a shift of the TSHR immunized mice bacterial communities described by the beta-diversity weighted Unifrac. Furthermore, we observed a significant positive correlation

between the presence of *Firmicutes* and orbital-adipogenesis specifically in TSHR-immunized mice.

Conclusions: The significant differences observed in microbiota composition from BALBc mice undergoing the same immunization protocol in comparable specific-pathogen free (SPF) units in different centers support a role for the gut microbiota in modulating the induced response. The gut microbiota might also contribute to the heterogeneity of induced response since we report potential disease-associated microbial taxonomies and correlation with ocular disease.

Keywords: Graves' orbitopathy; Graves' disease; Induced animal model; Gut microbiota; TSHR; Metataxonomics; Orbital adipogenesis; *Firmicutes.*

Background

The poor reproducibility of murine models of human diseases has become a puzzling phenomenon in recent decades. Apart from the genetic background of the strains used, the type of animal housing, diet and even the vendor can influence disease phenotype [1,2].

In Graves' disease (GD) and Graves' Orbitopathy (GO), *in vivo* models could help to unravel the pathogenetic mechanisms leading to autoimmunity and identify new therapeutic targets. [3]. The lack of spontaneous models of GD and GO necessitates induction of disease under laboratory conditions (reviewed in [4]).

Graves' disease is an organ-specific antibody-mediated autoimmune disease, governed by both genetic predisposition and environmental factors, in which thyroid-stimulating antibodies (TSAb) mimic the function of thyroid-stimulating hormone (TSH) to activate the thyrotropin receptor (TSHR). Moreover, the presence of thyroid-stimulating blocking antibodies (TSBAb), which inhibit the TSHR signaling cascade, and neutral antibodies to TSHR have been described in GD [5]. GD symptoms include hyperthyroidism, weight loss, heat intolerance and tremors; it affects about 2% of the population in the UK, with a female predominance. About 20% of GD patients develop an eye disease, Graves' orbitopathy or ophthalmopathy (GO), characterized by pro-inflammatory cells and tissue remodeling (extraocular muscle inflammation, adipogenesis, over-production of extra-cellular matrix) in the orbit [6].

Several GD mouse models have been developed using different immunization protocols with no signs of concomitant eye disease as previously reviewed [4,7-8]. Ludgate and colleagues established a TSHR-induced GO model by genetic immunization; i.e. injecting a TSHR expression plasmid [9]. Mice developed thyroiditis plus some aspects of GO and disease could be transferred to naive recipients using the TSHR-primed T cells from the genetically immunized mice. However, the model could not be reproduced in a different animal unit (neither was specific-pathogen free (SPF)) and the TSHR-induced disease was quite distinct

61 from that previously described, which the authors postulated might be due to microorganisms
62 [10]. It has also been reported that TSHR-immunized mice from a conventional environment
63 had higher and more persistent TSAb levels than mice in SPF units [11].
64 Recently, Berchner-Pfannschmidt and colleagues reported the induction of GO-like disease in
65 two independent SPF units [12]. The immunization protocol utilized genetic delivery of TSHR
66 A-subunit plasmid by close field electroporation, which leads to features of GD accompanied
67 by symptoms of eye disease, such as adipogenesis and inflammatory infiltrates in the orbit
68 [7,13]. Controls received a plasmid encoding the β-galactosidase (βgal) gene delivered by the
69 same procedure. Most aspects of the model were reproduced successfully, however, there was
70 heterogeneity in induced disease and differences in thyroid function in the animals undergoing
71 experimental GO in the two locations [12].
72 Over the years the gut microbiota has been associated with several diseases [14-17] and its
73 confounding role in establishing or reproducing disease phenotype in murine models has also
74 been proposed [18].
75 The murine model of multiple sclerosis, experimental autoimmune encephalomyelitis (EAE),
76 seems to be highly influenced by the gut microbiota. Oral antibiotic immunization and
77 consequent depletion of the gut bacteria, before disease induction, resulted in protection from
78 disease development, along with reduction in pro-inflammatory mediators such as IL-17 and
79 an increased Th2-immune response [19]. On the contrary, the intestinal monocolonization of
80 germ free mice (sterile) with segmented filamentous bacteria (SFB) restored the disease
81 phenotype, along with an increased number of Th17 cells in the CNS, suggesting a direct
82 interplay of the gut microbiota and the immune response in EAE development [20].
83 Based on these observations, we hypothesized that the gut microbiota itself might play a major
84 role not only in the establishment, but also in the reproducibility of the GO animal model
85 described above. The presence or absence not only of pathogens, but also of symbiotic and

commensal bacteria can favor an immune response more prone to inflammation and conducive to autoimmunity [21].

We aimed to characterize, for the first time, the gut microbiota of the GD/GO models via a combination of metataxonomics (16S rRNA gene sequencing) and traditional microbial culture approaches. We compared the gut contents of TSHR immunized mice from the two centers to understand whether variation in gut composition could explain differences in the disease induced. Within one center, we then characterized the gut microbiota between different immunizations (TSHR and βgal) and compared them with untreated mice, to determine whether the gut microbiota can influence the outcome and correlate with disease features.

Materials and methods

GO preclinical mouse model samples

Mouse samples used in the present work were obtained from a recent study [12], conducted in parallel in two independent animal housing units, under comparable SPF conditions. Animal procedures in center 1 were reviewed and approved by the Ethical Committee of King's College London and conducted with Personal and Project licenses under United Kingdom Home Office regulations. Animal procedures in center 2 were reviewed and approved by North Rhine Westphalian State Agency for Nature, Environment and Consumer Protection (LANUV), Germany. Samples from the animal unit of King's College London (UK) will be referred to as the "Center 1" and included a total of 5 TSHR-immunized mice (TSHR). Samples from the University of Duisburg-Essen (Germany) will be referred to as the "Center 2", including 10 TSHR-immunized (TSHR), 8 βgal plasmid controls (βgal) and 6 untreated mice (included as a background control), as shown in Table 1.

The GO immunization protocol has been previously described [13]. Briefly, 6-8 weeks old BALB/cOlaHsd female mice were immunized via intramuscular injection into each biceps

femoris muscle [22] and electroporation of either the eukaryotic expression plasmid pTriEx1.1Neo-hTSHR (hTSHR289) (TSHR group) or the control plasmid pTriEx1.1Neo-β-gal (plasmid-control, βgal group). All animals, whether TSHR or βgal controls, received a total of four plasmid injections at three week-intervals of the experiment (0, 3, 6, 9 weeks).

Each mouse was anesthetized using isoflurane with a properly calibrated vaporizer throughout the immunization procedure (injection and electroporation). After the immunization, mice were carefully transferred to a recovery cage until fully recovered.

Mice in Center 1 were maintained conventionally in open cages in one room and co-housed at a maximum of 3 animals per cage. In Center 2, the mice were co-housed according to their immunizations, 2-4 animals per individually ventilated cage in one room. All mice were provided by different outlets of the same supplier (Harlan Ltd or Harlan laboratories BV). In both centers, mice received autoclaved water and had been fed *ad libitum* similar commercial chow from different suppliers (Rat and Mouse no.1 Maintenance from Special Diet Services, LBS Biotech UK for Center 1 and Rat/Mouse Maintenance V1534-300 from Ssniff Spezialadiaten GmbH, Germany, for Center 2). Also the cage bedding was from different suppliers.

All immunized and control mice in both locations were sacrificed nine weeks after the last immunization (18 weeks) to permit the development of the chronic phase of the disease in the TSHR group (Additional file 1: Figure S1).

After sacrifice, murine intestines were snap-frozen and stored in sterile containers at −80°C. For subsequent analysis, whole intestines were thawed and directly afterwards placed on a sterile padding. The organs were dissected into two or three parts and the content of all parts was scratched out from oral to aboral end with a sterile inoculation loop resulting in one sample per mouse, which was collected in a sterile container and frozen at -80°C until needed. Within

the Center 2 only, fecal pellets of βgal and TSHR immunized mice were also collected before each injection (week 0, 3, 6, 9). Total DNA was extracted from fecal pellets as described below. Methods for: i) the evaluation of clinical symptoms, ii) the determination of the thyroid hormone thyroxine blood levels (fT4) and TRAB (both stimulating TSAb and blocking TSBAb) antibodies, iii) the measurement of the expansion of fat cells (adipogenesis) and muscular atrophy in the orbit have been already described [12]. A full description of the mice involved and samples collected in the present study is represented in Table 1.

Table 1 Description of the mouse groups involved in this study

No. of animals	Immunization	Centers	Source	Timepoint
5	TSHR	1	Intestinal scraping	T4
10	TSHR	2	I.S./Feces	T0-T4*
8	βgal	2	I.S./Feces	T0-T4*
6	Untreated	2	I.S./Feces	T4°

A total of 23 female BALB/cOlaHsd, 6-8 weeks old mice were challenged either with the pTriEx1.1Neo-hTSHR to induce disease (TSHR group) or with pTriEx1.1Neo-β-gal as a plasmid control group (βgal group). Independent SPF animal units were based in London (Center 1) and Essen (Center 2). An untreated group of 6 mice has been included as a background control. Samples collection comprised of intestine scraping (I.S.) from Center 1 and both fecal pellets and I.S. within the Center 2. *Fecal pellets of βgal and TSHR immunized mice have been collected before any immunization (T0) and during the time course of the immunization protocol until the sacrifice (T4), as represented in Additional file 1: Figure S1. °Untreated mice were sampled at T4 before (fecal) and after the sacrifice (intestinal scraping).

Traditional microbial cultures of mouse gut contents

A total of 29 scraped intestinal samples (Table 1) derived from Center 1 and Center 2 were analyzed. One gram of feces per mouse was diluted in 9 ml pre-reduced maximum recovery diluent (CM0733, Oxoid, Basingstoke, United Kingdom) with 20% v/v glycerol and the solution was mixed by vortexing for 5 s. Afterwards, 10-fold serial dilutions were prepared, and 100µl of each dilution was plated onto different culture media under aerobic or anaerobic conditions (Anaerobic Workstation, AW400SG, Elektrotek, Keighley, West Yorkshire, United Kingdom). Specific media, culture conditions and dilution used to isolate different bacteria are listed in Additional file 2.

Bacteria were identified by Gram staining, colony morphology, the presence of spores, catalase reaction and partially by the API system (BioMerieux, Marcy-l'Étoile, France). Viable bacterial cell counts were enumerated and all counts were recorded as the numbers of log 10 colony forming units per gram of sample. Counts data were Box-Cox transformed before statistical analysis [23]. Mouse groups were compared through the Analysis of variance (one-way ANOVA) and Tukey's multiple comparisons test with adjusted *P* values.

Extraction of total DNA from gut contents and feces and 16S rRNA gene sequencing

A total of 29 scraped intestinal samples and 96 fecal pellets were individually placed in 2mL tubes prefilled with 0.1mm silica and zirconia bead mix (Benchmark Scientific, Edison, USA), dissolved in 1mL InhibitEX buffer (Qiagen Ltd, West Sussex, UK) and vortexed until homogenized. A bead-beating step (Beadbug microcentrifuge homogenizer, Benchmark Scientific, USA) was applied for 3 x 60sec at 5m/s with 5 min rest in-between. The DNA extraction has been performed with QiAmp Fast DNA Stool Mini kit (Qiagen Ltd, UK), following the manufacturer's instruction. Total genomic DNA was eluted in sterile microcentrifuge tubes and quantified by Qubit Fluorimetric Quantitation (ThermoFisher Scientific Ltd, UK), following manufacturer's instructions. DNA aliquots were kept at -20°C until used. Sequencing of the variable regions of the 16S rRNA gene was performed at Research and Testing Laboratory LLC. (Lubbock, Texas, USA). Primers used to amplify the V1-V2 regions of 16S rRNA gene were: 28F (5'-GAGTTTGATCNTGGCTCAG-3') and 388R (5'-TGCTGCCTCCCGTAGGAGT-3'). Sequencing was performed using an Illumina Miseq (Illumina, San Diego, USA), with 10K paired-end sequencing protocol.

Processing and statistical analysis of metataxonomic data

Processing of the sequences was performed using Mothur v1.36, to reduce possible PCR effects and to cluster sequences into Operational Taxonomic Units (OTUs) at the 97% identity cut-off

and provide the taxonomic annotations [24]. Paired-end reads (R1 and R2) were joined for each sample using the Mothur function "make.contigs" and trimmed at the 2.5%-tile and 97.5%-tile on the distribution lengths of the amplicons. Sequences with any ambiguities (i.e. Ns) were removed by setting parameter N=0. Filtered sequences were aligned against the SILVA 16S rRNA gene reference database (http://www.arb-silva.de). Removal of chimera sequences was done with the Uchime tool [25]; singleton and non-bacterial sequences (e.g. *Archaea*, Eukaryotic, Chloroplast and Mitochondria) have been removed from the analysis. The taxonomic assignment from phylum to genus level of the processed sequences was done using the Ribosomal Database Project (RDP) Naïve Bayesian Classifier, using Trainset 14 with a cut-off of 80% [26]. FastTree (version 2.1.7) has been used to build a phylogenetic tree, using an approximated maximum likelihood solved by Jukes-Cantor evolutionary model [27]. To reduce the effect of possible different sampling methods and to obtain comparable sequencing libraries, each sample library has been subsampled based on the smallest library size. OTUs with less than 10 counts have been excluded from the dataset and grouped as "OTU_low", and the analysis has been performed collapsing OTUs at the phylum-genus levels. Statistical analysis was performed in R (Version 3.2.2) and STAMP tool for metataxonomic data analysis [28].

Alpha diversity indices (Observed OTUs, Chao1, ACE and Shannon) were calculated within samples from Mothur and tested for association with covariates (e.g. locations and immunizations) using a linear model, followed by Tukey's Honest Significant Difference (HSD) post-hoc analysis.

Beta diversity was estimated using the Unifrac weighted distance to compare bacterial communities among samples [29], and represented in a Non-Metric Dimensional Scaling (NMDS) plot. The permutational multivariate analysis of variance (PERMANOVA) was calculated through the Adonis function [30] in R Vegan package (using 999 permutations) and

was used to test the association between the microbiota composition and the covariates (e.g. location of the laboratories or immunizations).

The hierarchical clustering of genera was performed using the Spearman distance and the Ward agglomeration method. Statistical tests with $P \leq 0.05$ were considered as significant.

Over multiple timepoints, the effects of time, immunizations and their interactions, have been estimated on the fecal microbiota composition, all by means of the following linear model:

$$y_{ijk} = \mu + Time_i + Immunization_j + (Time * Immunization)_{ij} + e_{ijk}$$

where y is the vector of either alpha-diversity Chao or Shannon indices, or of the *Firmicutes/Bacteroidetes* ratio calculated from the relative abundances in each sample at each timepoint; μ is the overall mean; time is the effect of timepoint in classes (T0, T1…T4); immunization is the type of immunization (either the TSHR or βgal). The factorial interaction between immunization and time has also been included in the model; *e* is the vector of residual effects. Comparison between βgal and TSHR immunizations at each timepoint was made using the pairwise T-test with Benjamini-Hochberg correction for false rate discovery (FDR).

To test differences in phylum and genus counts between immunizations and timepoints, the same model was used in the generalized linear model (GLM) implemented in the EdgeR package [31]. Pairwise comparisons of phylum and genus counts between timepoints and immunizations have been assessed with Fisher's Exact Test in EdgeR package.

Correlations of either the taxonomy counts (phylum and genus relative abundances) or the microbial counts from the traditional culture approach and disease features, such as anti-TSHR antibodies and thyroid hormone thyroxine levels (fT4), orbital adipogenesis or muscular atrophy values, were estimated using the Spearman correlation coefficient (Rho) and represented in a correlation plot, using the R Corrplot package. Additional statistical methods are described in Additional file 2.

Results

Sequencing metrics

From 16S rRNA gene sequencing (V1-V2 regions), a total of 5,333,798 reads were obtained which reduced to 4,047,186 reads after quality filtering. Following alignment, we obtained an average of 20,534 reads per sample, ranging from 3,502 to 134,901. Subsampling per library size resulted in a 96% average coverage per OTU definition at 3,052 reads per sample. The averaged coverage and subsampling was sufficient to describe gut bacterial communities according to sequence-based rarefaction curves (data not shown).

We identified a total of 4,281 OTUs: 1,037 OTUs had more than 10 counts across samples, and were retained.

Comparative analysis of the gut microbiota of GO preclinical mouse models in different centers

To assess whether the microbiota has an impact on the GO mouse model in different laboratories, we compared the gut microbial contents of 5 TSHR mice from Center 1 and 10 TSHR immunized BALB/c female mice from Center 2, after sacrifice (T4).

Comparison of the alpha diversity indices showed a significant reduction in the richness (P=0.01), but not in the diversity of the Center 2 microbial community (P>0.05, Figure 1A). The gut microbiota composition from the two centers showed a good separation according to the Spearman distance and Ward hierarchical clustering (Figure 1B), and a PERMANOVA test on the weighted Unifrac distances revealed a spatial difference between bacterial communities (P=0.005 with 999 permutations, Figure 1C).

At a phylum level, *Bacteroidetes* and *Firmicutes* were the most represented of the 7 phyla identified, with no differences between them in the two centers (P=0.99). *Lactobacillaceae*, *Ruminococcaceae* and *Porphyromonadaceae* families were more abundant in Center 2 than in

Center 1 TSHR mice (P<0.01, Figure 1D). We observed significant differences in the abundance of eighteen genera between the two centers, as detailed in Table 2.

From the traditional microbial culture of the gut contents, we observed differences in yeasts (P=0.03186), *Bacteroides* (p<0.0005) and total anaerobes (P=0.00081) counts, which were found to be enriched in the Center 1 compared with the Center 2 TSHR mice (Table 3). Cultures from mouse intestinal scraping of the Center 2 did not contain any total clostridia, *Bacteroides* or yeasts, and we were able to culture enterobacteria, *E. coli* and coliforms from only one mouse from this group. *E.coli* and coliforms were also the least abundant in the Center 2 TSHR mice (Figure 1E). Furthermore, since *Yersinia enterocolitica* has been implicated in GD pathogenesis [32] we used selective agar plates for *Yersinia* sp. but no *Yersinia* colonies grew.

Table 2 Genera differentially abundant between Center 1 (n=5) and Center 2 (n=10) TSHR immunized mice intestinal scraped samples

Genera	Center 1: mean freq. (%)	Center 2: mean freq. (%)	*P* values
Allobaculum	1.001	0.003	0.042
Alloprevotella	6.135	0.432	0.003
Bacteroides	9.370	1.525	0.017
Bifidobacterium	0.668	0.006	0.003
Clostridium XI	0.840	0.000	0.005
Coprobacter	1.835	4.226	0.033
Fusicatenibacter	0.989	3.295	0.032
Guggenheimella	0.006	0.169	0.011
Helicobacter	0.200	0.000	0.024
Intestinimonas	0.097	0.861	0.000
Lactobacillus	2.304	18.632	0.030
Lactonifactor	0.023	0.401	0.025
Meniscus	1.149	0.000	0.000
Oscillibacter	0.640	1.748	0.011
Parabacteroides	0.292	0.031	0.015
Pseudoflavonifractor	0.154	0.466	0.028
Rikenella	3.921	1.216	0.004
Turicibacter	3.629	0.000	0.002

ANOVA with Tukey's HSD post-hoc analysis (95% confidence interval), generated with STAMP. Mean freq: mean frequency (%).

Table 3 Traditional microbiology results from TSHR-immunized mouse intestinal scraping from Center 1 (n=5) and Center 2 (n=10)

Microbial target	Center 1: mean counts	Center 2: mean counts	*P* values
Bacteroides	1.15E+05	b.d.l.	0.000
Bifidobacteria	6.41E+06	1.32E+06	0.057
Coliforms	3.27E+02	1.15E+03	0.453
E.coli	b.d.l.	8.45E+02	0.499
Enterobacteria	b.d.l.	6.82E+02	0.499
Enterococci	1.74E+05	6.10E+06	0.247
Lactobacilli	1.93E+06	4.68E+06	0.725
Staphylococci	1.31E+05	3.77E+05	0.175
Total aerobes	4.18E+05	9.90E+06	0.370
Total anaerobes	6.75E+06	7.39E+05	0.001
Total Clostridia	2.46E+04	b.d.l.	0.165
Yeast	8.72E+01	b.d.l.	0.031

b.d.l.: below detection limit. Detection limits are the following according to the agar used: 1000 CFU/g feces for *Bacteroides*, 100 CFU/g feces for *E.coli* and coliforms as well as for enterobacteria, and 10

CFU/g feces for total clostridia and yeasts, respectively. Microbiological counts were Box-Cox transformed. *P* values obtained by linear regression.

Gut microbiota differences in immunized and control mice within the Center 2

To observe the possible contribution of the gut microbiota in the disease, we compared the gut microbiota composition between immunization groups in mice within the Center 2. No significant differences were observed in alpha diversity indices among immunizations, apart from the Abundance-based Coverage Estimator (ACE) index between untreated and TSHR groups (Figure 2A, P=0.01). The ACE index relies on the presence of rare OTUs [33], which were more abundant in the untreated group compared to the plasmid-immunized mice. The βgal group showed a slightly skewed distribution of the Shannon index when compared to the others; however, the post-hoc comparison was not significant.

The non-metric dimensional scaling (NMDS) of the weighted Unifrac distances matrix showed a separation of the three immunization groups, also confirmed by the permutation test (P<0.01, 999 permutations; Figure 2B). βgal bacterial communities were closer to those of the untreated mice, while we observed a spatial shift of the TSHR immunized bacterial communities.

OTUs from *Bacteroidetes* and *Firmicutes* phyla were the most abundant among the phyla identified (Figure 2C) and showed a different distribution pattern among immunized groups. In particular, *Firmicutes* counts were higher in TSHR immunized mice (P=0.05) and *Bacteroidetes* were found to be higher in the untreated group (P=0.012). At a genus level, eight genera were differentially abundant between TSHR and βgal groups; three genera between TSHR and the untreated group and four genera between βgal and the untreated group (Additional file 3: Table S1). We found an enrichment of OTUs of *Acetitomaculum* genus in the βgal group compared to both TSHR (P=0.004) and the untreated group (P=0.003); an enrichment of *Lactobacillus* OTUs in the TSHR compared to the untreated group (P=0.018) and a reduction of *Bacteroides* counts in TSHR when compared to the βgal group (P=0.047). However, no significant differences were observed among immunized groups and in pairwise

304 comparisons generated by the traditional bacterial culturing approach (Additional file 3: Table
305 S2).
306 In the scraped intestinal samples, we did not observe a cage effect on the composition of the
307 large intestine microbiota (PERMANOVA P>0.05; Figure 2D).

308 **Dynamics of fecal microbiota during the immunization protocol**

309 To assess whether the immunization plasmids and the duration of the protocol could have
310 influenced the gut microbiota composition, we sequenced the bacterial 16S rRNA gene from
311 the fecal pellets of the βgal and TSHR group from the baseline (T0) for 18 weeks afterwards,
312 until the end of the experiment (T4).
313 We observed a significant increase of the richness (Chao index, figure 3A; P=0.02) and the
314 diversity (Shannon index, figure 3B) over time, which was less apparent in the TSHR
315 immunized group. Significant differences regarding of richness between TSHR and βgal have
316 been observed at T4 (P=0.027, Table 4). The Shannon index of diversity, on the contrary, was
317 significantly different between TSHR and βgal immunization at T1 (P=0.023, Table 4).

318 **Table 4** Summary of the statistics from the time-course analysis of the fecal microbiota during
319 the immunization protocol (T0-T4) and between immunizations (βgal and TSHR)
320

Index	ANOVA model			TSHR *vs.* βgal group				
	Immunization	Time	Time*Immunization	T0	T1	T2	T3	T4
Chao	0.006	0.02	0.8	0.75	0.066	0.28	0.33	0.027
Shannon	0.054	0.28	0.47	0.44	0.023	0.35	0.35	0.29
Firm:Bact	0.406	0.0003	0.16	0.39	0.028	0.46	0.2	0.26

321
322 Firm:Bact, *Firmicutes*/*Bacteroidetes* ratio. ANOVA model as previously described. Pairwise
323 comparison between βgal and TSHR in each time point has been made with a pairwise T-test with
324 Benjamini-Hochberg correction for FDR.
325

326 The murine fecal microbiota comprised *Bacteroidetes* and *Firmicutes* phyla predominantly
327 (Figure 4C); followed by *Tenericutes*, *Proteobacteria Deferribacteres* and Candidatus
328 Saccharibacteria phyla. The *Firmicutes*/*Bacteroidetes* ratio has been used to describe the shift
329 in the gut microbiota associated with ageing [34] and also in disease conditions such as obesity

[35]. The ratio showed differences amongst the timepoints of the experimental procedure (P<0.01) and between TSHR and the βgal group after three weeks from the first injection (T1, P=0.011; Figure 3C).

We fitted a generalized linear model (GLM) to compare the taxonomic counts at different timepoints within each group independently (either TSHR or βgal). Thirty-four genera have been identified as differentially abundant among all timepoints in the TSHR immunized group (Additional file 4: Table S1), while 25 were found in the βgal group (Additional file 4: Table S2). We observed differences in the taxonomic profile between TSHR and βgal groups at each timepoint using an exact test (EdgeR). Once again T1 was identified as the timepoint with the highest number of genera differentially expressed, as illustrated by the diversity indices (Additional file 4: Table S3).

In contrast to data obtained from the gut microbiota (Figure 2D), a cage effect was observed in the fecal microbiota, in particular, in interaction with time (P=0.001) and immunization (P=0.002; Additional file 5: Figure S1). The latter is probably due to the mice being caged according to the type of plasmid injection they received, but we also observed a significant difference within the same immunization group (e.g. TSHR in cage 4 and cage 5, P=0.01).

Correlating the gut microbiota composition with clinical features and differences in GO development

We then investigated possible correlations between disease features, such as anti-TSHR antibodies, thyroxine levels (fT4), orbital adipogenesis and muscular atrophy, and the gut microbiota composition to determine whether it contributes to the heterogeneity of induced responses, summarized in Additional file 1: Table S1.

Within the Center 1 TSHR-immunized group, we found that OTUs from *Firmicutes* and *Bacteroidetes* negatively correlated to each other (Rho=-1, P<0.0001). A positive correlation

between levels of TSAb and *Deferribacteres* phylum, which include one-genus *Mucispirillum*, was found (Rho=0.92, *P*=0.028; Figure 4A).

From those genera differentially abundant between TSHR-immunized mice from Center 1 and Center 2 (Table 2), identified via metataxonomics, we observed a strong negative correlation of the *Firmicutes* genus *Intestinimonas* and the levels of TSBAb in the Center 1 (Rho=-0.89, *P*<0.05), but not in the Center 2 counterpart (Figure 4B). No significant correlation was observed between OTUs from the genus *Intestinimonas* and levels of TSAb or levels of free thyroxine hormone (fT4; data not shown).

On the contrary, the Box-Cox transformed counts from the traditional microbiology did not show any significant correlation with the disease features described (data not shown).

Within the Center 2, *Bacteroidetes* and *Firmicutes* negatively correlated to each other (Rho=-0.99, *P*<0.0001; Figure 5A). We also found a significant positive correlation (Rho=0.6, *P*=0.009) between the OTUs from the *Firmicutes* and the orbital adipogenesis value and a negative correlation of this value with the phylum *Bacteroidetes* (Rho= -0.57, *P*=0.014). As expected, these correlations were specific to the TSHR immunized mice (Figure 5B). The correlation pattern we found (*Firmicutes* positively correlated, *Bacteroidetes* negatively correlated) was also recapitulated at the genus level. Among the genera of the *Firmicutes*, three, within the Clostridia family (*Butyricicoccus*, *Parvimonas* and *Fusibacter*) and the genus *Lactobacillus* were correlated positively with adipogenesis; while three *Bacteroidetes* genera (*Anaerophaga*, *Paraprevotella* and *Tannerella*) correlated negatively with the orbital adipogenesis values (Figure 5C).

A strong positive correlation (Rho=0.82, *P*=0.007) was observed between orbital adipogenesis and the total anaerobes counts obtained from the traditional microbial cultures of TSHR immunized mice, but not in the controls (Figure 5D). Moreover, from the traditional microbial cultures data, we observed correlations with other disease features, specifically in the TSHR

group. We observed strong positive correlations between the muscular atrophy values and the cluster of lactobacilli (Rho=0.74, *P*=0.03), enterococci (Rho=0.8, *P*=0.02), bifidobacteria (Rho=0.76, *P*=0.03) and coliforms (Rho=0.73, *P*=0.04). Levels of free thyroxine (fT4) were positively correlated with lactobacilli (Rho=0.64, *P*=0.05) and staphylococci (Rho=0.77, *P*=0.016).

Discussion

Animal models have been invaluable in dissecting the mechanisms causing loss of immune tolerance leading to autoimmune conditions such as GD. Thus, we aimed to test the hypothesis that the gut microbiota may affect both outcome and reproducibility of induced autoimmune disease, such as reported in the recent research article of Berchner-Pfannschmidt and co-workers [12].

We observed significant differences in the diversity and spatial organization of the gut microbiota of female TSHR-immunized BALBc mice in two independent SPF units. We also demonstrated disease-associated microbial taxonomies and correlation with ocular disease, suggesting that the gut microbiota have contributed to the heterogeneity of induced response in the two locations, which further supports our hypothesis.

Animals were maintained in similar conditions. We are confident that there were no infections ongoing at the moment of sampling, since animals in both centers were routinely tested for the presence of viruses, mycoplasma and parasites (see Additional File 1: Table S2); moreover, housing facilities had comparable SPF conditions. Animals were from the same supplier but in different countries (Harlan Ltd. for Center 1 and Harlan Lab. BV for Center 2), had received autoclaved water and had been fed similar commercial chow, with the exception that food pellets provided in Center 2 contained twice the amount of iodide compared to Center 1 food (see Additional File 1: Table S3). Although iodide excess can be associated with abnormal thyroid function, we do not consider that this dietary variation is enough to explain the results

(i.e. elevated thyroxine levels were apparent in the Center 1 but not in Center 2 mice). The effect of iodine has been studied in the NOD mouse which spontaneously develops autoimmune thyroiditis. Vecchiatti and colleagues [36] reported that excess iodine (0.2 mgs/mouse/day) increased the incidence and severity of disease; however, the BALB/c mice in our study did not display thyroiditis. A transgenic NOD mouse expressing the human TSHR-A subunit is able to develop antibodies to the human TSHR and this too is exacerbated by iodine excess [37] but at levels far greater than in the chow used in Centers 1 and 2. We also considered whether iodine could affect the gut microbiota, in view of its use as an antiseptic, but all the studies we found were in this context, rather than the effect of dietary iodine on symbionts. The importance of SPF conditions is indicated by a previous study which failed to reproduce a GO animal model, despite using mice from the same supplier and identical bedding, water and chow [10]. However even SPF may be inadequate since differences were found in the gut microbiota of C57BL/6 colonies bred in two different rooms of the same SPF facility [38], fortunately mice in our study were all housed in the same room.

Cage effects were apparent in the fecal microbiota results, which highlight the importance of studying the gut microbiota instead when comparing autoantigen (TSHR)-immunized and control mice, which is in the close proximity of the intestinal mucosa and the immune system, enabling us to explore its relationship with disease features.

We observed several disease-associated taxonomies; the abundance of the newly described butyrate-producing genus *Intestinimonas* [39] was reduced in the Center 1 group compared to Center 2 and correlated negatively with TSBAb. The *Intestinimonas species butyroproducens* has a unique ability to produce butyrate from lysine and is involved in the detoxification of Advanced Glycosylation End (AGE) products such as fructoselysin, which have been linked to type-1 diabetes [40], although we are unaware of any link between butyrate-producing bacteria and thyroid autoimmunity.

429 The TSHR immunized group developed some signs of GO and their gut microbiota had
430 increased OTUs of the phylum *Firmicutes* but decreased *Bacteroidetes* compared with
431 controls. This mirrors our preliminary data in human disease where we observed a dramatic
432 reduction in the *Bacteroides* genus in GD patients when they develop GO (INDIGO
433 publishable summary[a]).
434 We also obtained a positive correlation between several *Firmicutes* counts, such as *Clostridia*
435 and *Bacilli*, with orbital adipogenesis in Center 2 TSHR-immunized mice. Million and co-
436 workers have previously reported a positive correlation between OTUs from the *Firmicutes*
437 and weight-gain/obesity in both animal models and humans [41]. Interestingly, the role of the
438 genus *Lactobacillus* and its products in either triggering or protecting from adipogenesis has
439 been debated and seems to be species-specific.
440 In the present work, we could exclude a possible gain-of-weight relationship with the
441 adipogenesis value calculated in the orbit since no changes in mouse weights have been
442 observed during the development of the chronic phase of the disease (data not shown).
443 Furthermore, molecular mechanisms driving obesity and orbital adipogenesis may well be
444 different, since the latter is derived from the neural crest and the gut microbiota may have
445 varying effects on different fat depots [42].
446 Our time-course analysis revealed that time had a dramatic role in shaping the fecal microbiota
447 of the female mice which were 6-8 weeks-old at the outset and 24-26 weeks at the end of the
448 experiment, confirming the work of McCafferty and colleagues [43]. The richness and diversity
449 of βgal control mice increased with age but this was less apparent in TSHR immunized animals.
450 Significant differences in microbiota composition between control and TSHR immunizations
451 were most apparent 3 weeks after the first immunization, at the initiation of the induced
452 immune response.

Our control group comprised mice immunized with the βgal expression plasmid in which we observed a slight skew in the microbiota richness and diversity which may be caused by the systemic overexpression of the β-galactosidase enzyme, whose natural role is in glycan metabolism, e.g. the hydrolysis of the lactose to galactose and glucose [44]. Kaneda and collaborators reported a βgal overexpression peak in the muscle fibers following electroporation from five days to 2 weeks after the injection [45].

It may be that the increased OTUs of the *Firmicutes* genus *Acetitomaculum* was specifically triggered by the product of the βgal enzymatic reaction over time (Additional file 4: Table S2). This effect merits further investigation but we are confident that the βgal vector plasmid provides the optimum control group since its microbial communities were more closely related to that of the naïve non-immunized group than to TSHR immunized mice. Of interest, TSHR-immunized mice in Center 2 were more similar to TSHR-immunized mice from Center 1 (P=0.2) than βgal (P=0.024), than untreated (P=0.04) mice in their own center (Additional File 6: Figure S1).

The results we obtained using 16S rRNA gene metataxonomics and via the traditional microbial culture approach were largely similar, with relatively few differences. Microbial cultures revealed significantly higher yeast counts (P=0.03186) in Center 2 TSHR immunized mice - which obviously could not be seen via the bacterial metataxonomics - and a nearly significant difference in the *Actinobacteria* genus *Bifidobacterium* (P=0.057), which was not detected in our metataxonomics data. Primers based on the V1-V2 regions of the 16S rRNA gene did not detect *Bifidobacterium* OTUs. Consequently, we applied a new set of primers (28F-combo) with which we observed a significant enrichment of bifidobacteria counts in the Center 2 (Additional file 7: Figure S1), in agreement with the microbial culture results.

Conclusions

In conclusion, our results indicate a role for the gut microbiota in modulating the heterogeneity apparent in the TSHR-induced model of GD and GO. In our next study we will report the effects on our induced model of modifying the gut microbiota using antibiotics, probiotics and fecal material transfer.

Our future studies will investigate whether the presence, absence or amounts of certain bacteria or yeast have the ability to directly alter the immune balance between the Treg anti-inflammatory response and the Th17-mediated pro-inflammatory response in the gut mucosa as has been reported in models of other autoimmune diseases [22,46]. Results of these experiments could then be confirmed by colonization studies in gnotobiotic animals. Factors such as level of dietary iodine intake and age of mice at immunization, which may both alter the gut microbiota and/or immune responsiveness, are also warranted.

Figure legend

Fig. 1 Comparative analysis of the gut microbiota in independent animal units. **a** Box and whisker plot of the alpha diversity indices for richness (Chao1 and observed OTUs indices) and evenness (Shannon index) of the bacterial communities in TSHR immunized mice housed in Center 1 (blue) and Center 2 (red), respectively. Tukey's HSD post-hoc: Chao1, P=0.01; Observed OTUs, P<0.001; Shannon, P=0.08. **b** Annotated heatmap based on Spearman distance and Ward hierarchical clustering of the top 30 genera shows how well the two locations cluster together. Taxonomy explanation includes genera, family and phylum, which are entered in order of abundance. Genus abundance is described by the change in the intensity of the grey color, as annotated. **c** Multidimensional scaling plot (MDS) based on the weighted Unifrac distances between the two animal units. PERMANOVA with 999 permutations P=0.005. **d** Differentially abundant family from a pairwise comparison with Welch's t-test with 95% confidence intervals (STAMP). **e** Box and whisker plot culture results from intestinal scraped samples derived from TSHR-immunized mice from Center 1 and Center 2. Results are expressed as a Log(x+1) transformed colony-forming-units/gram feces (cfu/g). P-values: * P<0.05; ** P<0.001; *** P<0.005.

Fig. 2 Gut microbiota composition in TSHR immunized mice and control mice in Center 2 at final timepoint. **a** Box and whisker plot describing the measurement of alpha diversity (Chao, ACE and Shannon indices). **b** Non-metric dimensional scaling (NMDS) plot of weighted Unifrac distances showed a spatial separation of microbial communities according to the immunizations. PERMANOVA based on 999 permutations P=0.001. **c** Boxplot of the phylum counts according to immunizations. ANOVA on phylum counts BH adjusted P<0.0001 and pairwise T-test between *Bacteroidetes*-*Firmicutes* counts adjusted P=0.0003. **d** Non-Metric Dimensional Scaling (NMDS) plot based on weighted Unifrac distances shows spatial separation of the microbial community according to the immunization and caging within the Center 2. Mice were co-housed according to their immunization at a maximum of 4 animals; cages are described by different shapes as in the legend. No significant difference in cage effect is observed. PERMANOVA based on cage effect (999 permutations) for all comparisons P=0.12. P-values: * $P\leq$0.05; ** P=0.01.

Fig. 3 Time-course analysis of GO preclinical fecal microbiota during the immunization protocol. Box and whisker plot of alpha diversity such as Chao, **a**, and Shannon, **b**, indices showed differences over time. **c** Phylum dynamics over time and between immunizations. *Firmicutes* and *Bacteroidetes* were the most abundant phyla, showing differences with time and immunizations. Significant differences among timepoints have been observed at the *Firmicutes/Bacteroidetes* ratio, in particular between the baseline T0 and the last timepoint T4, but not related to immunization. A significant difference in the ratio was observed after three weeks from the first injection (T1) between βgal and TSHR. P-values: * $P\leq$0.05; ** P=0.01.

Fig. 4 Correlating the gut microbiota and disease features in Center 2 TSHR group. **a** Spearman correlation coefficient strength (Rho) of phylum counts from TSHR mice in Center 2. *Firmicutes* and *Bacteoridetes* showed a strong negative correlation between each other. A positive correlation between the one-genus phylum *Deferribacteres* and the level of thyroid-stimulating antibodies (TSAb) has been observed. Correlations with P<0.05 are shown and strength of the Rho coefficient is represented by the change in the colour intensity. fT4, free thyroid hormone thyroxine levels; TSAb, thyroid stimulating antibodies; TSBAb, thyroid-stimulating blocking antibodies (as a percentage values). **b** Enriched

Firmicutes genus *Intestinimonas* between Center 1 (blue) and Center 2 (red) showed a strong negative correlation with the percentage of thyroid-stimulating blocking antibodies (TSBAbs) at 95% confidence interval in Center 1 (Rho=-0.8, P=0.04), but not in Center 2.

Fig. 5 Correlation of the gut microbiota composition with clinical features and differences in Center 2 mice. **a** Correlation plot of phyla and the orbital adipogenesis value. Spearman correlation coefficient strength (Rho) as indicated by the colored bar. Firmicutes and *Bacteoridetes* showed a strong negative correlation between each other. A positive correlation between *Firmicutes* and a negative correlation with *Bacteroidetes* OTUs and the adipogenesis value (calculated in the orbit) has been observed. Adipogenesis clustered closer to the Firmicutes and Bacteroidetes value according to the complete linkage method for hierarchical clustering. Only P<0.05 are shown. **b** Positive strong correlation of the *Firmicutes/Bacteroidetes* ratio with the adipogenesis value (calculated in the orbit) resulted significant in TSHR immunized group but not in the βgal group. **c** Spearman correlation coefficient (Rho) of genera among phyla *Bacteroidetes* and *Firmicutes* and the orbital adipogenesis values. The strength of the correlation coefficient is represented on x-axis: bars on the left represent a negative correlation coefficient, while bars on the right represent a positive correlation coefficient. Correlations with P<0.05 are shown; order of entrance depends on their P values: * P<0.05; ** P<0.1; *** P<0.005. **d** Spearman correlation coefficient plot of the Box-Cox transformed microbiological counts and disease features in Center 2 TSHR immunized mice. Features clustering was according to the complete linkage method for hierarchical clustering. Only correlations with P<0.05 are shown and strength of the correlation coefficient is represented by the change in the color intensity. fT4, free thyroid hormone thyroxine levels; TSAb, thyroid stimulating antibodies; TSBAb, thyroid-stimulating blocking antibodies (as a percentage values).

List of Abbreviations

ACE, abundance-based coverage estimator

AGE, advanced glycosylation end

βgal, β-galactosidase enzyme

CNS, central nervous system

EAE, experimental autoimmune encephalomyelitis

FDR, false rate discovery

fT4, thyroid hormone thyroxine

GD, Graves' disease

GLM, generalized linear model

GO, Graves' orbitopathy or ophthalmopathy

HSD, honest significant difference

NMDS, non-metric dimensional scaling

OTU, operational taxonomic unit

PERMANOVA, permutational multivariate analysis of variance

RDP, ribosomal database project

SFB, segmented filamentous bacteria

SPF, specific-pathogen free

TRAB, thyroid-stimulating hormone autoantibodies

Treg, regulatory T cells

TSAb, thyroid-stimulating antibodies

TSBAb, thyroid-stimulating blocking antibodies

TSH, thyroid-stimulating hormone

TSHR, thyrotropin receptor

Declarations

Ethics approval
The study was approved by the North Rhine Westphalian State Agency for Nature, Environment and Consumer Protection, Germany and by the Ethics Committee of King's College London, United Kingdom (UK).

Consent for publication
Not applicable.

Availability of data and material
The datasets used and/or analyzed during the current study are available from the corresponding author on reasonable request, since we are waiting for the repository accession number.

Competing interests
None of the authors declare any conflicting interests in the manuscripts.

Funding
Supported by Marie-Sklodowska Curie Industry Industry-Academia Pathways and Partnerships (IAPP) action, GA number 612116 project INDIGO. Deutsche Forschungsgemeinschaft grant BE3177/2–1 (UBP). Internal KCL funds (JPB).

Authors' contributions
SM collected the data, was involved in writing the report with GM and HLK. GM analyzed the data with FB and JRM. HLK, DC, JPB, UBP, MH, SDC, GEG, SP and AE contributed to study design and samples collection. ML designed and managed the project, supervised analyses and contributed to the report. All authors read and agreed to the final version of the manuscript.

Acknowledgements
We acknowledge the work of the other members of the INDIGO consortium: Mario Salvi, Lei Zhang, Giuseppe Colucci, Daryn Michael and Iveta Garaiova. We also acknowledge the invaluable help of Dr. Ann Smith.

Additional files

Additional file 1: Figure S1. Schematic representation of the GO immunization protocol and sample collection. **Table S1.** Summary of disease characteristics induced in mice in Center 1 and Center 2 using TSHR expression plasmid illustrating the heterogeneity of response. **Table S2.** Quarterly Health Screen Reports on viral, bacterial, mycoplasma and parasite screen in both centers. **Table S3.** Composition of the commercial chows provided *ad libitum* in Center1 and Center2. (DOCX)

Additional file 2: Supplementary methods. (DOCX)

Additional file 3: Table S1. Differential abundant taxonomic analysis between TSHR (n=10), βgal (n=8) and untreated (n=6), within Center 2. Welch's T-test with 95% confidence interval using STAMP. Mean relative frequency, rel. freq. Standard deviation, std. dev. **Table S2.** Comparison of intestinal scraped samples from different immunization within Center 2 from the traditional microbiological culture. Data were Box-Cox transformed. (XLSX)

Additional file 4: Table S1. Generalized linear model (GLM) of genera counts differentially present in TSHR immunized mice over timepoints, in reference to the baseline (T0) using EdgeR. LogFC, Log2 fold change between each timepoint and the baseline (T0); LR, likelihood ratio. **Table S2.** Generalized linear model (GLM) of genera counts in βgal control mice over timepoints using EdgeR. LogFC, Log2 fold change between each timepoint and the baseline (T0); LR, likelihood ratio. **Table S3.** Pairwise comparison of TSHR and βgal mice using Fisher's Exact Test in EdgeR at each timepoint (T0 to T4). LogFC, Log2 fold change of βgal compared to TSHR. (XLSX)

Additional file 5: Figure S1. Temporal stability of fecal microbiota and cage effect of the immunizations. Weighted Unifrac distances of mice fecal microbial communities represented over the time course of the experiment according to the immunization (**A**) or the cage (**B**). Permutational MANOVA of weighted Unifrac distances according to timepoint, immunizations, caging and their interactions (time x cage; time x immunization; immunization x cage) as described in Additional file 2. The time had a significant effect on the stability of the fecal microbiota (P=0.001), in particular between the baseline (T0) and the last timepoint (T4, P=0.003); and between the T1 and T4 (P=0.009). The interaction between time and immunization was significant (P=0.007). Cage was also significant, in particular the interaction cage x timepoint (P=0.001) and cage x immunization (P=0.002). Significant differences within the same immunization group cage has been observed (TSHR group in C4 and C5, P=0.01). (PDF)

Additional file 6: Figure S1. NMDS plot based on the weighted Unifrac distances of Center2 immune and control mice including TSHR-immunized mice from Center 1. TSHR-immunized mice from Center 1 were more similar to TSHR-immunized mice from Center 2 (P=0.2) than to the βgal (P=0.024) than the untreated (P=0.04). (PDF)

Additional file 7: Figure S1. *Bifidobacterium* counts derived from the 28F-combo primers in the TSHR immunized mice in Center 1 (n=5) and Center 2 (n=10). ANOVA with Tukey's HSD post-hoc analysis (95% confidence interval), P value=0.003 generated with STAMP. (PDF)

Endnotes

[a] INDIGO publishable summary: http://www.indigo-iapp.eu/publishable-summary/

References

1. Ericsson AC, Davis JW, Spollen W, Bivens N, Givan S, et al. Effects of vendor and genetic background on the composition of the fecal microbiota of inbred mice. PloS One. 2015; 10, e0116704.
2. Hufeldt MR, Nielsen DS, Vogensen FK, Midtvedt T, Hansen AK. Variation in the gut microbiota of laboratory mice is related to both genetic and environmental factors. Compar Med. 2010;60:336–47.
3. Draman M, Ludgate M. Thyroid eye disease- an update. Exp Rev Ophthalmol. 2016;11:1–12.
4. McLachlan SM, Rapoport B. Breaking tolerance to thyroid antigens: changing concepts in thyroid autoimmunity. Endocr Rev. 2014;35:59–105.
5. Morshed SA, Davies TF. Graves' disease mechanisms: The role of stimulating, blocking and cleavage region TSHR receptor antibodies. Horm Metab Res. 2015;47 Suppl 10:727-734.
6. Bahn RS. Graves' ophthalmopathy. New Engl J Med. 2010;362:726-738.
7. Banga JP, Moshkelgosha S, Berchner-Pfannschmidt U, Eckstein A. Modelling Graves' orbitopathy in experimental Graves' disease. Horm Metab Res. 2015; http://dx.doi.org/10.1055/s-0035-1555956.
8. Ludgate M. Animal models of Graves' disease. Eur J Endocrinol. 2000; 142:1-8.
9. Many MC, Costagliola S, Detrait M, Denef JF, Vassart G, Ludgate M. Development of an animal model of autoimmune thyroid eye disease. J Immunol. 1999;162**:**4966–4974.
10. Baker G, Mazziotti G, Ruhland C von, Ludgate M. Reevaluating thyrotropin receptor-induced mouse models of Graves' disease and ophthalmopathy. Endocrinology. 2005;146:835-844.
11. Bhattacharyya et al, 2005; from Contemporary endocrinology: Autoimmune Diseases in Endocrinology, Weetman AP, Humana Press, 2008
12. Berchner-Pfannschmidt U, Moshkelgosha S, Diaz-Cano S, Edelmann B, Görtz G-EE, Horstmann M, et al. Comparative assessment of female mouse model of Graves' orbitopathy under different environments, accompanied by pro-inflammatory cytokine and T cell responses to thyrotropin hormone receptor antigen. Endocrinology. 2016;en20151829.
13. Moshkelgosha S, So P-W, Deasy N, Diaz-Cano S, Banga J. Retrobulbar Inflammation, Adipogenesis, and Acute Orbital Congestion in a Preclinical Female Mouse Model of Graves' Orbitopathy Induced by Thyrotropin Receptor Plasmid-in Vivo Electroporation. Endocrinology. 2013;154:3008–3015.
14. Murri M, Leiva I, Gomez-Zumaquero JM, Tinahones FJ, Cardona F, et al. Gut microbiota in children with type 1 diabetes differs from that in healthy children: a case-control study. BMC Med. 2013;11:46.
15. Brown CT, Davis-Richardson AG, Giongo A, Gano KA Crabb DB, et al. Gut microbiome metagenomics analysis suggests a functional model for the development of autoimmunity for type 1 diabetes. PloS One. 2011;6: 25792.
16. Frank DN, St. Amand AL, Feldman RA, Boedeker EC, Harpaz N, Pace NR. Molecular-phylogenetic characterization of microbial community imbalances in human inflammatory bowel disease. 2007; Proc Natl Acad Sci U S A 104: 13780-13785.
17. Scanlan PD, Shanahan F, O'Mahony C, Marchesi JR. Culture-independent analyses of temporal variation of the dominant fecal microbiota and targeted bacterial subgroups in Crohn's disease. J Clin Microbiol. 2006;44:3980-3988.
18. Laukens D, Brinkman BM, Raes J, De Vos M, Vandenabeele P. Heterogeneity of the gut microbiome in mice: guidelines for optimizing experimental design. FEMS Microbiol Rev. 2016;40:117-132.

19. Ochoa-Repáraz J, Mielcarz DW, Ditrio LE, Burroughs AR, Foureau DM, et al. Role of gut commensal microflora in the development of experimental autoimmune encephalomyelitis. J Immunol. 2009;183:6041-6050.
20. Lee YK, Menezes JS, Umesaki Y, Mazmanian SK. Proinflammatory T-cell responses to gut microbiota promote experimental autoimmune encephalomyelitis. Proc Natl Acad Sci U S A. 2011;108 Suppl 1:4615-4622.
21. Covelli D, Ludgate M. The thyroid, the eyes and the gut: a possible connection. J Endocrinol Invest. 2017; DOI 10.1007/s40618-016-0594-6.
22. Zhao SX, Tsui S, Cheung A, Douglas RS, Smith TJ, Banga JP. Orbital fibrosis in a mouse model of Graves' disease induced by genetic immunization of thyrotropin receptor cDNA. J Endocrinol. 2011;210:369 –377.
23. Box GEP, Cox DR. An analysis of transformations. J R Stat Soc B 1964;26:211–243.
24. Schloss PD, Westcott SL, Ryabin T, Hall JR, Hartmann M, et al. Introducing mothur: open-source, platform-independent, community-supported software for describing and comparing microbial communities. Appl Environ Microbiol. 2009; doi:10.1128/AEM.01541-09.
25. Edgar RC, Haas BJ, Clemente JC, Quince C, Knight R. UCHIME improves sensitivity and speed of chimera detection. Bioinformatics. 2011;27:2194-2200.
26. Cole JR, Wang Q, Cardenas E, Fish J, Chai B, et al. The Ribosomal Database Project: improved alignments and new tools for rRNA analysis. Nucl Acids Res. 2009;37:D141-D145.
27. Price MN, Dehal PS, Arkin AP. FastTree 2–approximately maximum-likelihood trees for large alignments. PloS One. 2010;5:e9490.
28. Parks DH, Tyson GW, Hugenholtz P, Beiko RG. STAMP: statistical analysis of taxonomic and functional profiles. Bioinformatics. 2014; doi:10.1093/bioinformatics/btu494.
29. Lozupone C, Lladser ME, Knights D, Stombaugh J, Knight R. UniFrac: an effective distance metric for microbial community comparison. ISME J. 2011;5:169-172.
30. Anderson MJ. A new method for non-parametric multivariate analysis of variance. Austral Ecol. 2001;26:32-46.
31. Robinson MD, McCarthy DJ, Smyth GK. edgeR: a Bioconductor package for differential expression analysis of digital gene expression data. Bioinformatics. 2010; doi:10.1093/ bioinformatics/btp616.
32. Köhling HL, Plummer SF, Marchesi JR, Davidge KS, Ludgate M. The microbiota and autoimmunity: Their role in thyroid autoimmune diseases. Clin Immunol. 2017; doi: 10.1016/j.clim.2017.07.001.
33. Chao A. Species estimation and application. In: Kotz S, Balakishnan N et al., editors. Encyclopedia of statistical sciences. New York: Wiley; 2005. p. 7907-7915.
34. Mariat D, Firmesse O, Levenez F, Guimarães VD, Sokol H, et al. The Firmicutes/Bacteroidetes ratio of the human microbiota changes with age. BMC Microbiol. 2009;9:123.
35. Ley RE, Turnbaugh PJ, Klein S, Gordon JI. Microbial ecology: human gut microbes associated with obesity. Nature. 2006; 444:1022-1023
36. Vecchiatti S, Guzzo M, Caldini E, Bisi H, Longatto-Filho A, et al. Iodine increases and predicts incidence of thyroiditis in NOD mice: histopathological and ultrastructural study. Exp and therap med. 2013; 5:603–607
37. Rapoport B, Aliesky HA, Banuelos B, Chen C-RR, McLachlan SM. A unique mouse strain that develops spontaneous, iodine-accelerated, pathogenic antibodies to the human thyrotrophin receptor. J. Immunol. 2015; 194:4154–61
38. Jakobsson H, Rodríguez-Piñeiro A, Schütte A, Ermund A, Boysen P, et al. The composition of the gut microbiota shapes the colon mucus barrier. Embo Rep. 2015;16:164–177.

39. Kläring K, Hanske L, Bui TPN, Charrier C, Blaut M, et al. *Intestinimonas butyriciproducens* gen. nov., sp. nov., a butyrate-producing bacterium from the mouse intestine. Int J Syst Evol Microbiol. 2013; DOI: 10.1099/ijs.0.051441-0.
40. Bui TPN, Ritari J, Boeren S, Waard P de, Plugge CM, Vos WM. Production of butyrate from lysine and the Amadori product fructoselysine by a human gut commensal. Nat Commun. 2015;6:10062.
41. Million M, Lagier JC, Yahav D, Paul M. Gut bacterial microbiota and obesity. Clin Microb Inf. 2013;19:305–313.
42. Anderson DJ, Axel R. Molecular probes for the development and plasticity of neural crest derivatives. Cell. 1985;42(2):649–662.
43. McCafferty J, Mühlbauer M, Gharaibeh R, Arthur J, Perez-Chanona E, et al. Stochastic changes over time and not founder effects drive cage effects in microbial community assembly in a mouse model. ISME J. 2013;7:2116–2125.
44. Juers DH, Matthews BW, Huber RE. LacZ galactosidase: structure and function of an enzyme of historical and molecular biological importance. Protein Sci. 2012;21:1792–1807.
45. Kaneda T, Honda A, Hakozaki A, Fuse T, Muto A, Yoshida T. An improved Graves' disease model established by using in vivo electroporation exhibited long-term immunity to hyperthyroidism in BALB/c mice. Endocrinology; 2007;148:2335–44.
46. Wu H-J, Ivanov I, Darce J, Hattori K, Shima T, et al. Gut-Residing Segmented Filamentous Bacteria Drive Autoimmune Arthritis via T Helper 17 Cells. Immunity. 2010;32:815-827.

Fig 1

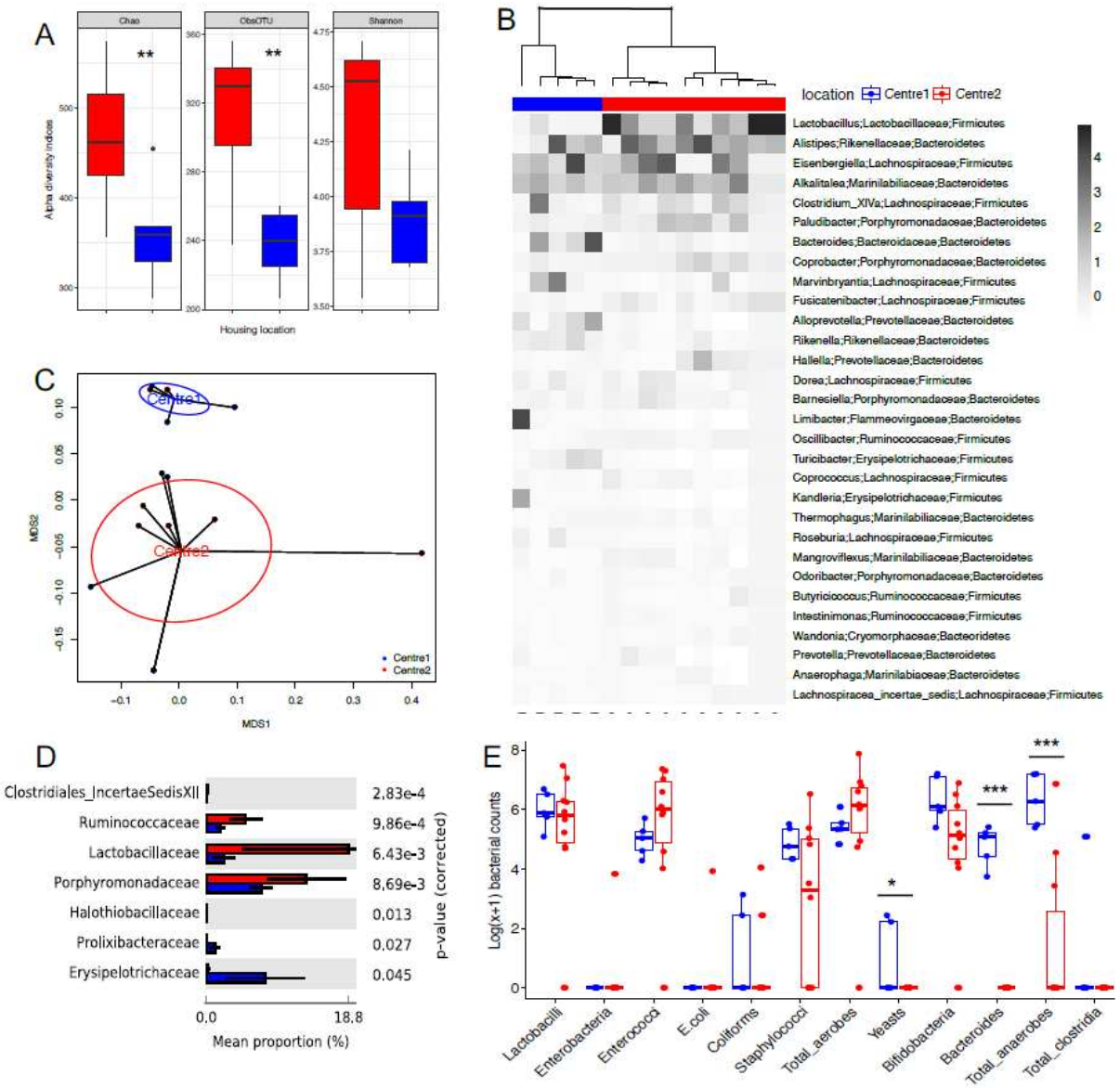
A
Chao
ObsOTU
Shannon
**
**
Alpha diversity indices
Housing location
B
location Centre1 Centre2
Lactobacillus;Lactobacillaceae;Firmicutes
Alistipes;Rikenellaceae;Bacteroidetes
Eisenbergiella;Lachnospiraceae;Firmicutes
Alkalitalea;Marinilabiliaceae;Bacteroidetes
Clostridium_XlVa;Lachnospiraceae;Firmicutes
Paludibacter;Porphyromonadaceae;Bacteroidetes
Bacteroides;Bacteroidaceae;Bacteroidetes
Coprobacter;Porphyromonadaceae;Bacteroidetes
Marvinbryantia;Lachnospiraceae;Firmicutes
Fusicatenibacter;Lachnospiraceae;Firmicutes
Alloprevotella;Prevotellaceae;Bacteroidetes
Rikenella;Rikenellaceae;Bacteroidetes
Hallella;Prevotellaceae;Bacteroidetes
Dorea;Lachnospiraceae;Firmicutes
Barnesiella;Porphyromonadaceae;Bacteroidetes
Limibacter;Flammeovirgaceae;Bacteroidetes
Oscillibacter;Ruminococcaceae;Firmicutes
Turicibacter;Erysipelotrichaceae;Firmicutes
Coprococcus;Lachnospiraceae;Firmicutes
Kandleria;Erysipelotrichaceae;Firmicutes
Thermophagus;Marinilabiliaceae;Bacteroidetes
Roseburia;Lachnospiraceae;Firmicutes
Mangroviflexus;Marinilabiliaceae;Bacteroidetes
Odoribacter;Porphyromonadaceae;Bacteroidetes
Butyricicoccus;Ruminococcaceae;Firmicutes
Intestinimonas;Ruminococcaceae;Firmicutes
Wandonia;Cryomorphaceae;Bacteroidetes
Prevotella;Prevotellaceae;Bacteroidetes
Anaerophaga;Marinilabiaceae;Bacteroidetes
Lachnospiracea_incertae_sedis;Lachnospiraceae;Firmicutes
C
Centre1
Centre2
MDS2
MDS1
Centre1
Centre2
D
Clostridiales_IncertaeSedisXII
Ruminococcaceae
Lactobacillaceae
Porphyromonadaceae
Halothiobacillaceae
Prolixibacteraceae
Erysipelotrichaceae
2,83e-4
9,86e-4
6,43e-3
8,69e-3
0,013
0,027
0,045
p-value (corrected)
0,0
18,8
Mean proportion (%)
E
Log(x+1) bacterial counts
Lactobacilli
Enterobacteria
Enterococci
E.coli
Coliforms
Staphylococci
Total_aerobes
Yeasts
Bifidobacteria
Bacteroides
Total_anaerobes
Total_clostridia

Fig 2

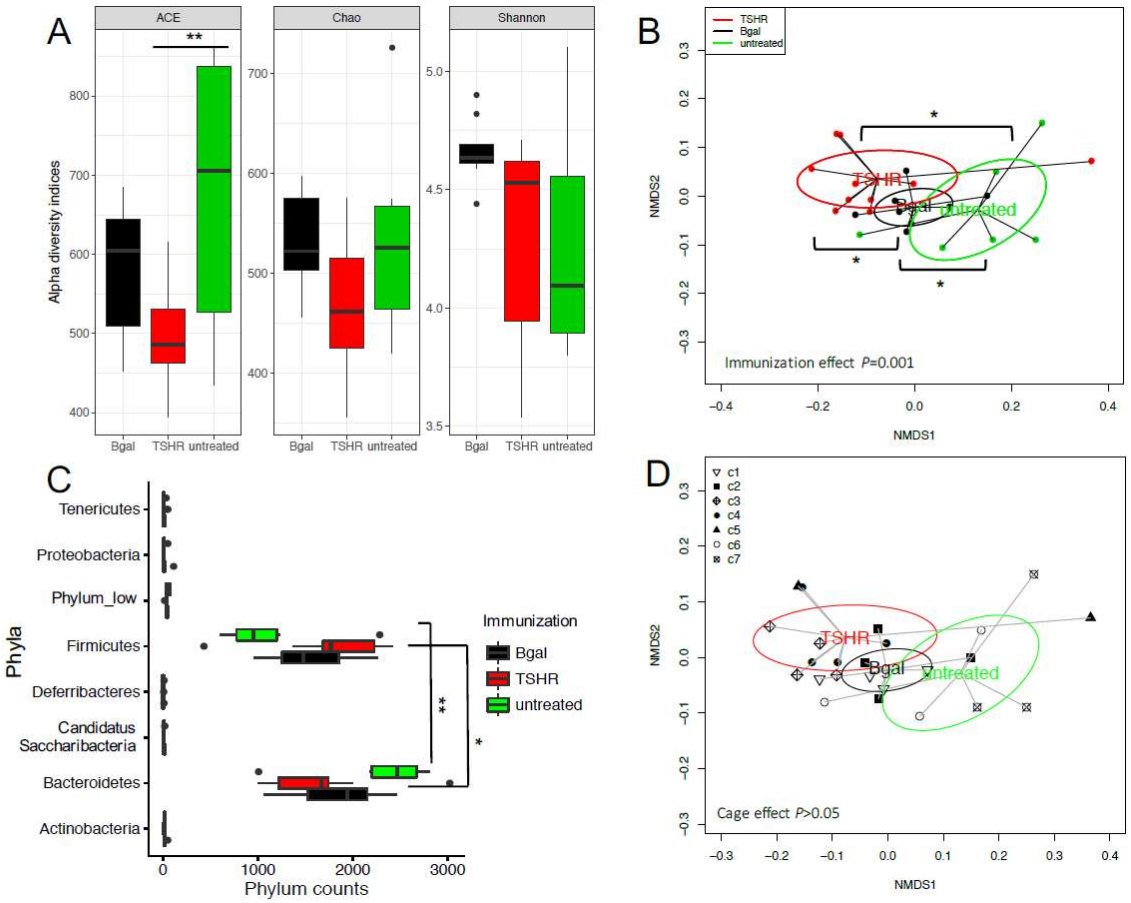
A
ACE
Chao
Shannon
Alpha diversity indices
Bgal
TSHR
untreated
B
TSHR
Bgal
untreated
NMDS1
NMDS2
Immunization effect P=0.001
C
Tenericutes
Proteobacteria
Phylum_low
Firmicutes
Deferribacteres
Candidatus Saccharibacteria
Bacteroidetes
Actinobacteria
Phyla
Phylum counts
Immunization
D
c1
c2
c3
c4
c5
c6
c7
Cage effect P>0.05

Fig 3

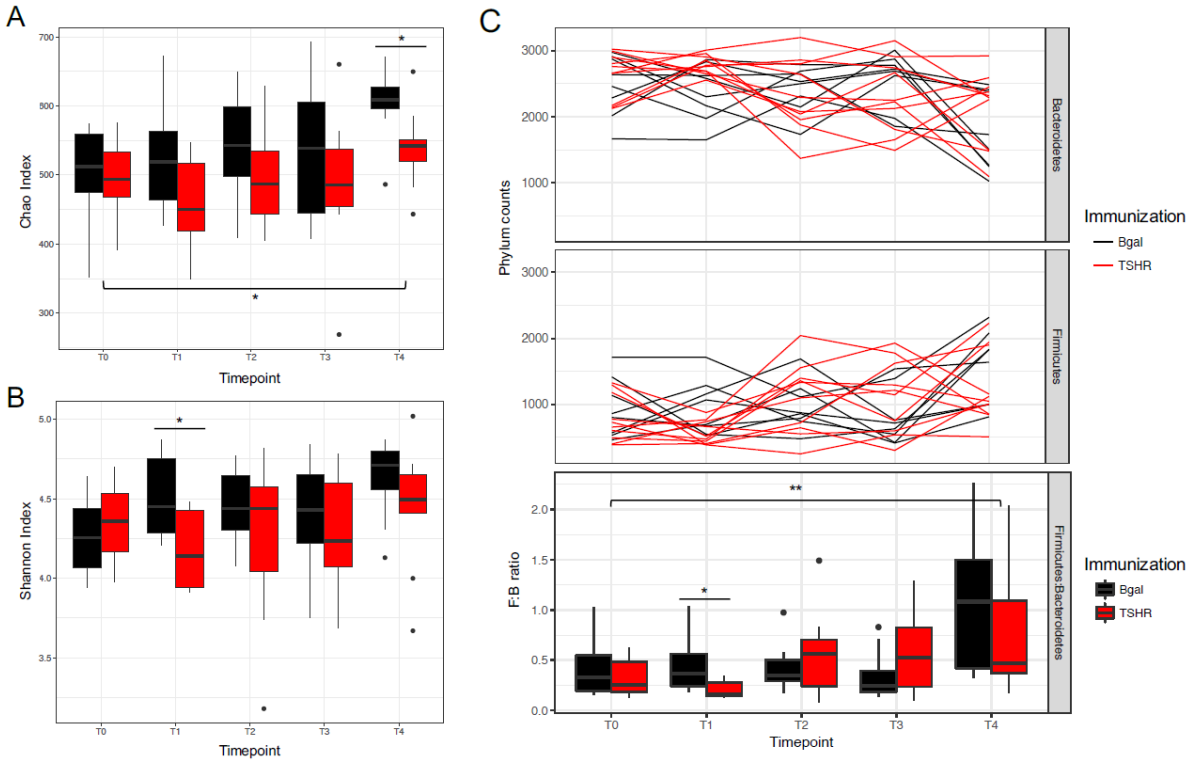
A
Chao Index
Timepoint
T0
T1
T2
T3
T4
B
Shannon Index
Timepoint
C
Phylum counts
Bacteroidetes
Firmicutes
F:B ratio
Firmicutes:Bacteroidetes
Timepoint
Immunization
Bgal
TSHR

Fig 4

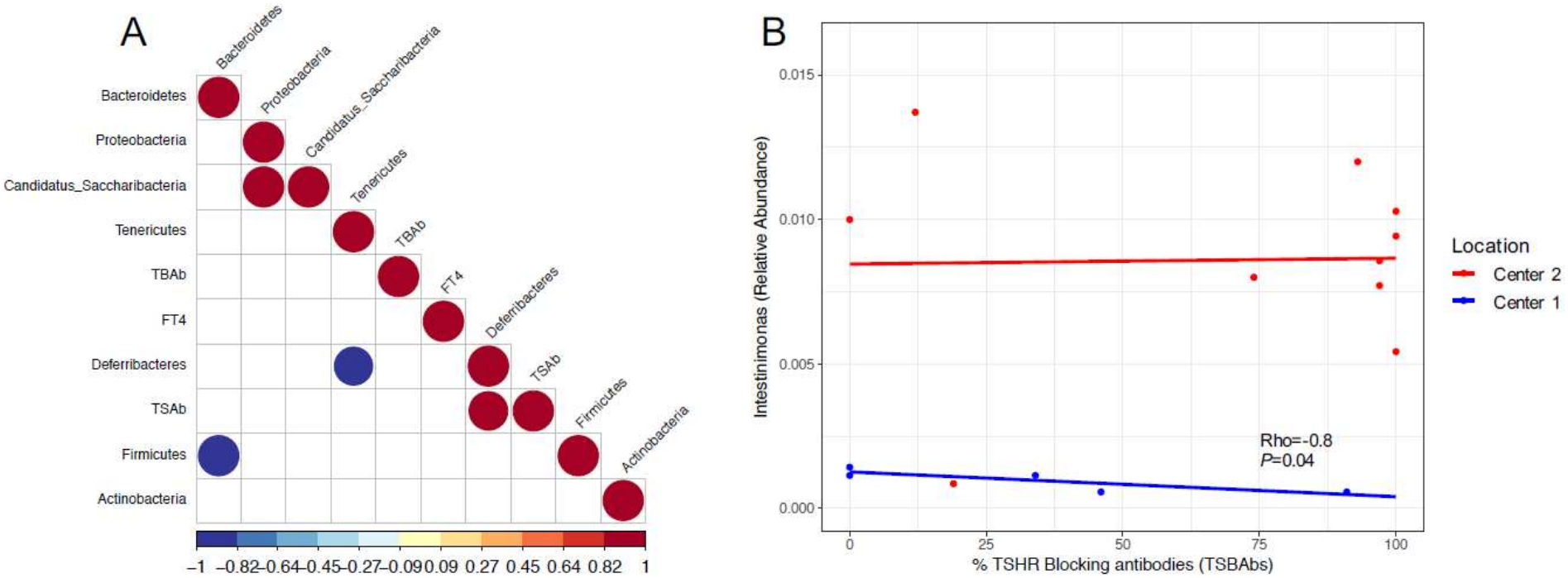
A
Bacteroidetes
Proteobacteria
Candidatus_Saccharibacteria
Tenericutes
TBAb
FT4
Deferribacteres
TSAb
Firmicutes
Actinobacteria
–1 –0.82 –0.64 –0.45 –0.27 –0.09 0.09 0.27 0.45 0.64 0.82 1
B
Intestinimonas (Relative Abundance)
0.015
0.010
0.005
0.000
0
25
50
75
100
% TSHR Blocking antibodies (TSBAbs)
Rho=-0.8
P=0.04
Location
Center 2
Center 1

Fig 5

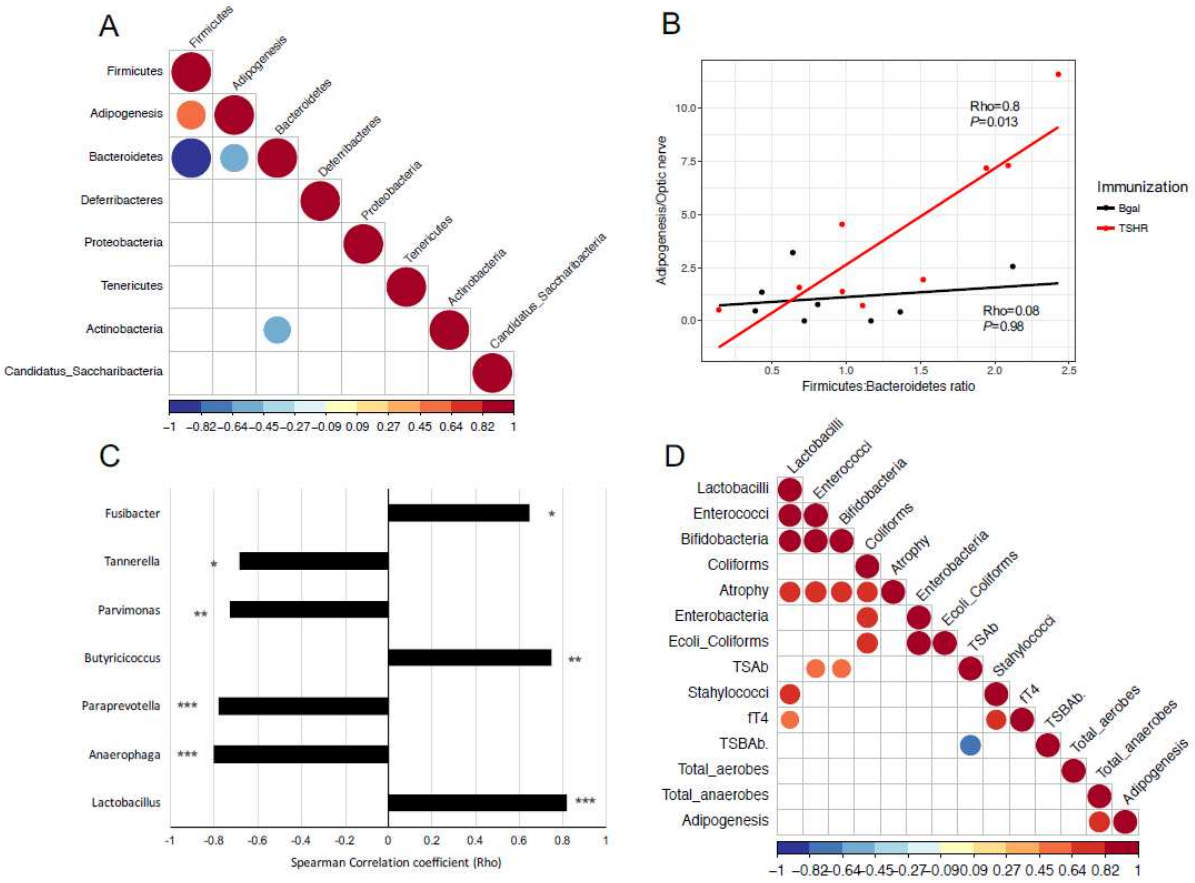
A
Firmicutes
Adipogenesis
Bacteroidetes
Deferribacteres
Proteobacteria
Tenericutes
Actinobacteria
Candidatus_Saccharibacteria
−1 −0.82 −0.64 −0.45 −0.27 −0.09 0.09 0.27 0.45 0.64 0.82 1
B
Rho=0.8
P=0.013
Rho=0.08
P=0.98
Adipogenesis/Optic nerve
Firmicutes:Bacteroidetes ratio
Immunization
Bgal
TSHR
C
Fusibacter
Tannerella
Parvimonas
Butyricicoccus
Paraprevotella
Anaerophaga
Lactobacillus
Spearman Correlation coefficient (Rho)
D
Lactobacilli
Enterococci
Bifidobacteria
Coliforms
Atrophy
Enterobacteria
Ecoli_Coliforms
TSAb
Stahylococci
fT4
TSBAb.
Total_aerobes
Total_anaerobes
Adipogenesis

Additional file 1

Figure S1

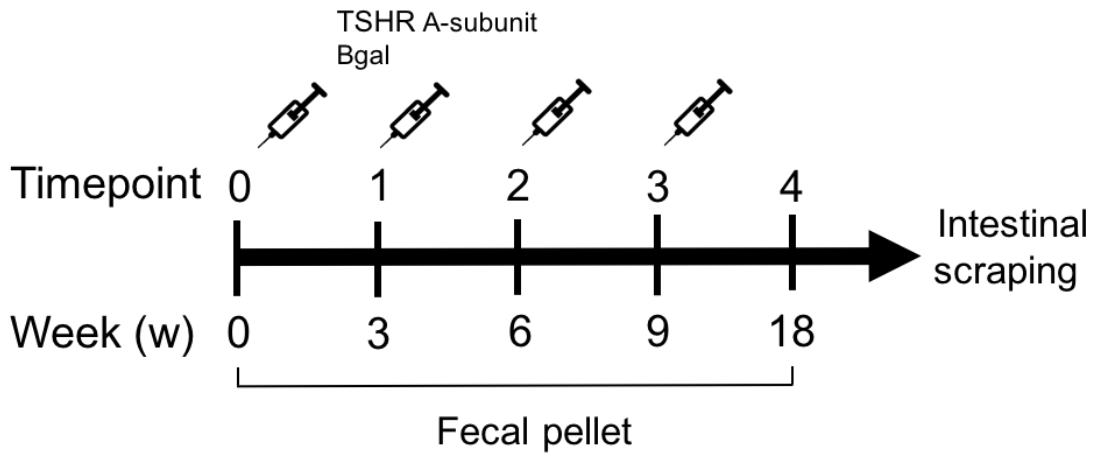

Schematic representation of the GO immunization protocol and sample collection. Female BALB/cOlaHsd, 6-8 weeks old mice were immunized via intramuscular injection and electroporation of either the eukaryotic expression plasmid pTriEx1.1Neo-hTSHR (hTSHR289) to develop signs of GO (TSHR A-subunit) or the control plasmid pTriEx1.1Neo-β-gal, as a plasmid-control group (βgal). Each animal received a total of four plasmid injections at three week-intervals. All immunized and control mice were sacrificed 9 weeks after the last immunization to permit the development of the chronic phase of the disease in the TSHR immunized group. Fecal pellets have been collected during the time course of the immunization trial from the baseline (T0) and before any other injection until the end of the procedure (T4). After euthanasia, the microbial content residing on the colonic mucosa has been collected through scraping.

Additional file 2

Supplementary methods

Media and conditions for microbial cultures

The following media, culture conditions and dilutions were used to isolate different bacteria in this study: Horse blood agar (Horse blood agar base No.2 (CM0271) with added Defibrinated Horse Blood (SR0050); both Oxoid, Basingstoke, United Kingdom) was incubated under aerobic conditions for 24 hours at 36 +/- 1 °C. Dilutions from 10^{-2} to 10^{-7} were made and total cell count was measured. MacConkey agar No. 3 (CM0115, Oxoid, Basingstoke, United Kingdom) was incubated under aerobic conditions for 24 hours at 36 +/- 1 °C. Dilutions from 10^{-2} to 10^{-7} were made and *Enterobacteriaceae (*red colonies with bile precipitation and straw coloured colonies) were counted. Slanetz and Bartley Medium (CM0377, Oxoid, Basingstoke, United Kingdom) was incubated under aerobic conditions for 24 hours at 36 +/- 1 °C. Dilutions from 10^{-2} to 10^{-7} were prepared and enterococci (deep red coloured colonies) were counted. Brilliance *E. coli* / coliform selective agar (CM1046, Oxoid, Basingstoke, United Kingdom) was incubated under aerobic conditions for 24 hours at 36 +/- 1 °C. Dilutions from 10^{-2} to 10^{-7} were made and *E. coli* (purple colonies) were counted. Tergitol 7 agar (CM0793, Oxoid, Basingstoke, United Kingdom) was incubated under aerobic conditions for 24 hours at 36 +/- 1 °C. Dilutions from 10^{-2} to 10^{-7} were prepared and coliforms (any color) were counted. Baird Parker agar base (CM0275, Oxoid, Basingstoke, United Kingdom) with added 50 ml of Egg Yolk Tellurite Emulsion (SR0054, Oxoid, Basingstoke, United Kingdom) was incubated under aerobic conditions for 48 hours at 36 +/- 1 °C. Dilutions from 10^{-2} to 10^{-7} were made and *Staphylococcus aureus* (black, shiny colonies with white and clear zones) were counted. Anaerobe basal agar (CM0972, Oxoid, Basingstoke, United Kingdom) was pre-reduced and incubated under anaerobic conditions for 48 hours at 36 +/- 1 °C. Dilutions from 10^{-2} to 10^{-7} were prepared and total cell count was measured. Each colony was checked for aerobic growth and ignored if so. Dichloran Rose-Bengal Chloramphenicol Agar (DRBC agar) (CM0727, Oxoid, Basingstoke, United Kingdom) was incubated under aerobic conditions for 48

hours at 36 +/- 1 °C. Dilutions from 10^{-1} to 10^{-2} were made and total yeast cell count was measured. Wilkins-Chalgren anaerobe agar (Code: CM0619, Oxoid, Basingstoke, United Kingdom) with added 1 vial of G-N Anaerobe Supplement (SR0108) and 25 ml defibrinated blood (SR0050/SR0051, both Oxoid, Basingstoke, United Kingdom) was pre-reduced and incubated under anaerobic conditions for 48 hours at 36 +/- 1 °C. Dilutions from 10^{-3} to 10^{-8} were made and *Bacteroides* spp. (grey/white colonies partially mucoid and with tattered edges) were counted. Each colony was checked for aerobic growth and ignored if so. MRS agar (CM0361, Oxoid, Basingstoke, United Kingdom) with added 1 vial of polymyxin B supplement (SR0099, Oxoid, Basingstoke, United Kingdom) was pre-reduced and incubated under anaerobic conditions for 48 hours at 36 +/- 1 °C. Dilutions from 10^{-3} to 10^{-8} were prepared and lactobacilli (pale straw coloured colonies) were measured. MRS-X agar (see MRS agar added 0.25 g L-cysteine hydrochloride monohydrate, 1 g Lithium chloride and 1.5 g Sodium propionate dissolved in 500 ml deionised water) was pre-reduced and incubated under anaerobic conditions for 48 hours at 36 +/- 1 °C. Dilutions from 10^{-3} to 10^{-8} were made and checked for bifidobacteria (small, shiny colonies). Alcohol shock anaerobe basal agar was prepared as follows: 1 ml of the 1 g faeces diluted in 9 ml maximum recovery diluent with glycerol was mixed with 1 ml ethanol (≥98%, Sigma Aldrich, St. Louis, Missouri, USA) and rolled for 30 min. Conditions were similar to anaerobe basal agar. Dilutions from 10^{-1} to 10^{-4} were made and total cell count was measured. Each colony was checked for aerobic growth and ignored if so.

Stability of the faecal microbiota over time

The function Adonis [Anderson, 2001] implemented in the Vegan package was used to test the variations between-samples of the microbial communities (calculated using the weighted Unifrac distance) over timepoints and among cages, via a permutational analysis of variance or non-parametric MANOVA. The linear predictors and response matrix were as following:

$$y_{ijk} = \mu + T_i + I_j + (T * I)_{ij} + C_k + (C * T)_{ki} + (C * I)_{kj} + e_{ijk}$$

whereas:

y_{ijk} is the weighted Unifrac matrix for treatment *i*, time *j* and cage *k*,

μ is the overall mean;

T_i is the effect of the *i*th time which was set as a class (T0, T1…T4);

I_j is the type of *j*th immunization which is represented by either TSHR or βgal;

C_k is the effect of *k*th cage which is expressed as a class (C1, C2…C5);

$(TI)_{ij}$ $(CT)_{ki}$ and $(CI)_{kj}$ represent factorial interactions between time, immunizarions and cage;

e_{ijk} is the vector of the residual effects.

A pairwise interaction within immunizations, cages and timepoints has been assessed using a built-in pairwise PERMANOVA script in R.

Additional File 3 Table S1

Comparison	Genus	mean rel. freq. (%)	std. dev. (%)	mean rel. freq. (%)	std. dev. (%)	difference between means	*P* value
TSHR *vs*. Bgal	Acetitomaculum	0.085566836	0.067504249	0.2852081	0.129133521	-0.199641264	0.004050551
	Bacteroides	1.52043332	0.853337957	3.429600304	2.05523723	-1.909166984	0.046774268
	Fusibacter	0.039939699	0.038703067	0.007129617	0.012348858	0.032810082	0.035281823
	Genus_low	1.075302786	0.24891733	1.372480403	0.263024859	-0.297177617	0.036977948
	Lachnobacterium	0.316582459	0.238402725	0.620236086	0.303623692	-0.303653627	0.048649574
	Parabacteroides	0.031372369	0.045019329	0.07842986	0.034197543	-0.047057491	0.030341303
	Parasporobacterium	0.330871338	0.157904043	0.13901992	0.13777991	0.191851418	0.019845227
	Peptococcus	0.085578215	0.075492454	0.367221557	0.300765541	-0.281643342	0.043112267
TSHR *vs*. untreated	Flavonifractor	0.128351482	0.066581061	0.04267177	0.048485122	0.085679711	0.016159478
	Lactobacillus	18.59136704	13.88312945	5.048233808	3.731541414	13.54313324	0.018575293
	Thiofaba	0.034233564	0.033267177	0.004748338	0.010617607	0.029485226	0.031091947
Bgal *vs*. untreated	Acetitomaculum	0.2852081	0.129133521	0.07120383	0.056310395	0.21400427	0.002863369
	Alloprevotella	0.156809908	0.287892738	1.344091904	0.872651646	-1.187281996	0.027430733
	Caminicella	0.053459424	0.052246474	0	0	0.053459424	0.030322651
	Flavonifractor	0.16040369	0.081786875	0.04267177	0.048485122	0.11773192	0.009190405

Additional File 3 Table S2

Microbial target	Average counts TSHR	Average counts βgal	Average counts untreated	*P* value	Bgal *vs*. TSHR	Bgal *vs*. untreated	TSHR *vs*. untreated
Bacteroides	0	0	3.64E+03	0.231	>0.999	0.289	0.259
Bifidobacteria	1.32E+06	4.89E+05	1.32E+06	0.57	0.788	0.909	0.559
Coliforms	1.15E+03	4.75E+03	5.43E+06	0.231	>0.999	0.289	0.259
E.coli and Coliforms	8.45E+02	6.04E+03	8.15E+06	0.935	0.988	0.974	0.928
Enterobacteria	6.82E+02	5.49E+03	5.88E+06	0.934	0.989	0.973	0.928
Enterococci	6.10E+06	5.10E+06	2.71E+06	0.461	0.509	0.999	0.593
Lactobacilli	4.68E+06	5.76E+05	9.44E+05	0.538	0.747	0.918	0.533
Staphylococci	3.77E+05	4.76E+07	2.36E+06	0.804	0.908	0.792	0.952
Total aerobes	9.90E+06	5.37E+06	1.53E+07	0.936	0.982	0.981	0.931
Total anaerobes	7.39E+05	1.95E+04	4.53E+06	0.675	0.661	0.828	0.98
Total Clostridia	0	0	1.36E+02	0.231	>0.999	0.289	0.259
Yeast	0	0	4.55E+00	0.231	>0.999	0.289	0.259

Additional File 4 Table S1

Genera	FC.TreatTSHR.Tim	FC.TreatTSHR.Tim	FC.TreatTSHR.Tim	FC.TreatTSHR.Tim	LR	P value
Thermophagus	0.285177093	0.207913239	-0.441964274	-1.478653366	21.70787	0.000229
Clostridium_IV	-1.422222292	1.038231619	0.091621959	1.777803588	21.20731	0.000288
Parvimonas	-0.319842898	-1.04675752	-1.920989583	-3.002927848	20.13822	0.000469
Galenea	4.526610618	-0.76182652	0.578601444	1.051732241	18.87745	0.000831
Propionibacterium	0	4.937135876	0	0	18.2622	0.001097
Robinsoniella	-3.029219391	-0.150474529	-1.602329317	-1.039113081	16.51914	0.002396
Parasutterella	0.673807925	-0.136523859	-0.27532242	-1.322923964	16.24971	0.002702
Anaerotruncus	-0.940567401	0.399244121	0.422073628	1.162379686	15.92644	0.003119
Fusicatenibacter	-0.476201227	1.111200473	1.395596494	1.421166964	15.23736	0.004233
Lactobacillus	-0.30482909	0.401067629	1.04950301	-0.797857951	15.1589	0.004383
Clostridium_XlVa	-0.802730637	0.274874964	0.962624849	1.222009171	15.07324	0.004552
Oxalophagus	-3.353406046	-4.26922455	-4.26922455	-4.26922455	14.90317	0.004906
Acetitomaculum	-0.585779617	0.871120683	1.258746299	2.018818479	14.89083	0.004933
Peptococcus	0.747086999	2.027229015	1.522765867	3.253626361	14.72086	0.005317
Mangroviflexus	-0.108881598	-1.143439812	-2.140539541	-1.320138436	14.28695	0.006433
Lachnoanaerobaculum	-1.881882649	-0.133200204	-0.721423174	1.821932971	13.55477	0.00886
Ruminococcus2	-0.558021392	0.190997913	0.61162587	1.672610439	13.53783	0.008926
Allisonella	-1.760941757	-1.760941757	-1.760941757	1.124762136	12.5405	0.013754
Salinihabitans	2.545298959	0.172505451	0.577341924	-1.947897767	12.50821	0.013946
Lacticigenium	-1.37549872	-1.37549872	-1.37549872	0.945546347	12.06197	0.016896
Sporobacterium	-4.299344588	-2.923529369	-4.299344588	-2.227786095	11.88361	0.018238
Limibacter	-0.246017903	-0.634743582	-1.005314908	-1.29561737	11.18601	0.024551
Cerasibacillus	-1.24541047	-2.717293243	-2.717293243	-1.340320006	10.95173	0.027112
Lactonifactor	-0.1603798	0.139021192	0.003717107	1.584167837	10.83909	0.028433
Alkalitalea	0.049006492	-0.341419418	-0.422229149	-0.918302384	10.73861	0.029664
Butyrivibrio	-1.438686773	0.483671973	0.941397989	0.222557658	10.44887	0.033509
Alistipes	0.098319716	0.157980939	0.689621786	0.889163018	10.33247	0.035185
Wandonia	-0.164579033	-0.242840127	0.882071545	0.671626541	10.31672	0.035417
accharibacteria genera incertae sed	-1.308315404	-0.765104903	-0.637814989	0.761031291	10.29135	0.035796
Lachnospiracea incertae sedis	-1.3035228	-0.583402961	-0.488594304	0.518977896	10.21334	0.036983
Papillibacter	-0.474675223	-0.245182463	-1.432619608	0.486013048	9.730153	0.045227
Paludibacter	0.020609251	-0.378688829	-0.558067558	-0.772128667	9.670426	0.046361
Acetanaerobacterium	0.51052216	0.577871811	1.182647973	2.433198839	9.545561	0.048819
Escherichia/Shigella	0	1.376087791	0.844761915	4.086564788	9.539523	0.048941

Additional File 4 Table S2

Genera	logFC.TreatBgal.TimeT1	logFC.TreatBgal.TimeT2	logFC.TreatBgal.TimeT3	logFC.TreatBgal.TimeT4	LR	*P* value
Parvimonas	-0.042493158	-1.133888162	-1.042337303	-4.125125753	20.74141658	0.000356325
Clostridium_IV	0.820586267	1.232731249	1.125797253	2.831499701	20.498407	0.000398061
Acetitomaculum	0.785799074	1.613733676	0.95590517	3.143592791	20.43178046	0.000410326
Lachnobacterium	0.877963226	1.314595669	-0.074523445	2.214209537	18.70129655	0.000899565
Lactobacillus	1.73034537	0.44862848	2.030410891	1.165476536	16.70710811	0.002203303
Thermophagus	-0.007798599	-0.084368503	-0.084381784	-1.668544936	16.21973299	0.002738052
Lactonifactor	-0.072618538	0.059932003	-0.459000887	1.973921533	16.21694668	0.00274145
Lachnoanaerobaculum	0.509757657	-0.003921067	-0.115093428	3.128679383	15.18915763	0.00432455
Guggenheimella	-0.941447029	-1.237053099	-0.728875446	-2.010743608	14.88219073	0.004951903
Robinsoniella	-1.001083904	-1.647733488	-2.756456618	-2.412938165	14.85200929	0.00501821
Mucispirillum	2.131574114	-0.74340622	-0.556031863	1.819015693	14.03805333	0.00717459
Anaeroplasma	3.709998461	2.770873903	2.564886589	4.626225648	13.0073238	0.011240064
Galenea	3.937208584	3.167466556	1.172143734	-1.324461377	12.15045764	0.0162668
Thermoflavimicrobium	-0.587531928	-2.174656654	-3.171797589	-3.171797589	11.52126126	0.021290071
Pelagibacterium	-1.876679109	-1.877140687	-1.137002093	-3.460504121	11.28328706	0.023558135
Parasporobacterium	0.154642835	-1.903193056	-0.770112429	-2.219743371	11.14977063	0.024931376
Erysipelotrichaceae_incertae_sedis	-0.905981398	-2.160276071	-0.814444665	-2.262186784	10.90922778	0.027603335
Parasutterella	0.592179714	0.591236624	-0.32120834	-0.963596371	10.90230974	0.027684137
Coprobacter	0.015158791	-0.043568054	0.220826836	-0.863857772	10.83810979	0.028444968
Eisenbergiella	-0.37474419	-0.265021463	-0.931552097	0.775950914	10.74198045	0.029622078
Rikenella	-0.679577207	-1.47599999	-0.351126529	-1.018677395	10.59067298	0.031570651
Butyrivibrio	0.802929201	0.269156058	-1.712918919	-0.343212354	10.11525143	0.038530398
Lachnospiracea_incertae_sedis	0.363075193	0.475212368	-1.070048175	1.010970904	10.11318565	0.03856364
Parabacteroides	1.427903837	1.112243408	0.151313213	0.124221955	9.964064748	0.041037377

Additional File 4 Table S3

Timepoint	Genera	logFC (Bgal vs. TSHR)	*P* value
T0	Guggenheimella	-1.593418277	0.00297182
	Peptococcus	-2.61417971	0.01946611
	Lactobacillus	1.343235012	0.02457758
T1	Robinsoniella	-3.065507327	0.00121532
	Clostridium_IV	-2.723185741	0.00359156
	Butyrivibrio	-2.293363835	0.00664856
	Mucispirillum	-2.774289292	0.01337697
	Prevotella	-8.903507981	0.01633615
	Acetitomaculum	-2.115372411	0.01786363
	Anaerovorax	-1.790900672	0.01789099
	Lachnospiracea incertae sedis	-1.516884723	0.02359936
	Faecalibacterium	-3.087910293	0.02649594
	Intestinimonas	-1.217734963	0.04031738
	Lachnobacterium	-1.347969782	0.04486279
T2	Parasporobacterium	2.640927285	0.00751542
	Parabacteroides	-1.46702779	0.01559129
	Lactobacillus	1.295658361	0.02923859
	Galenea	-3.574369446	0.04585986
	Barnesiella	-0.970464856	0.04922042
T3	Papillibacter	-2.487132887	0.00059914
	Butyrivibrio	2.602585108	0.00293209
	Marvinbryantia	1.871309072	0.00492323
	Butyricimonas	-1.491880466	0.02258578
	Ruminococcus	-2.242503921	0.03066274
T4	Lachnobacterium	-1.725906219	0.00670026
	Acetitomaculum	-1.868432268	0.0202365
	Parasporobacterium	2.233031643	0.02213694
	Coprobacter	0.772319802	0.02242843
	Clostridium IV	-1.533580692	0.03270514

Additional file 5: Figure S1

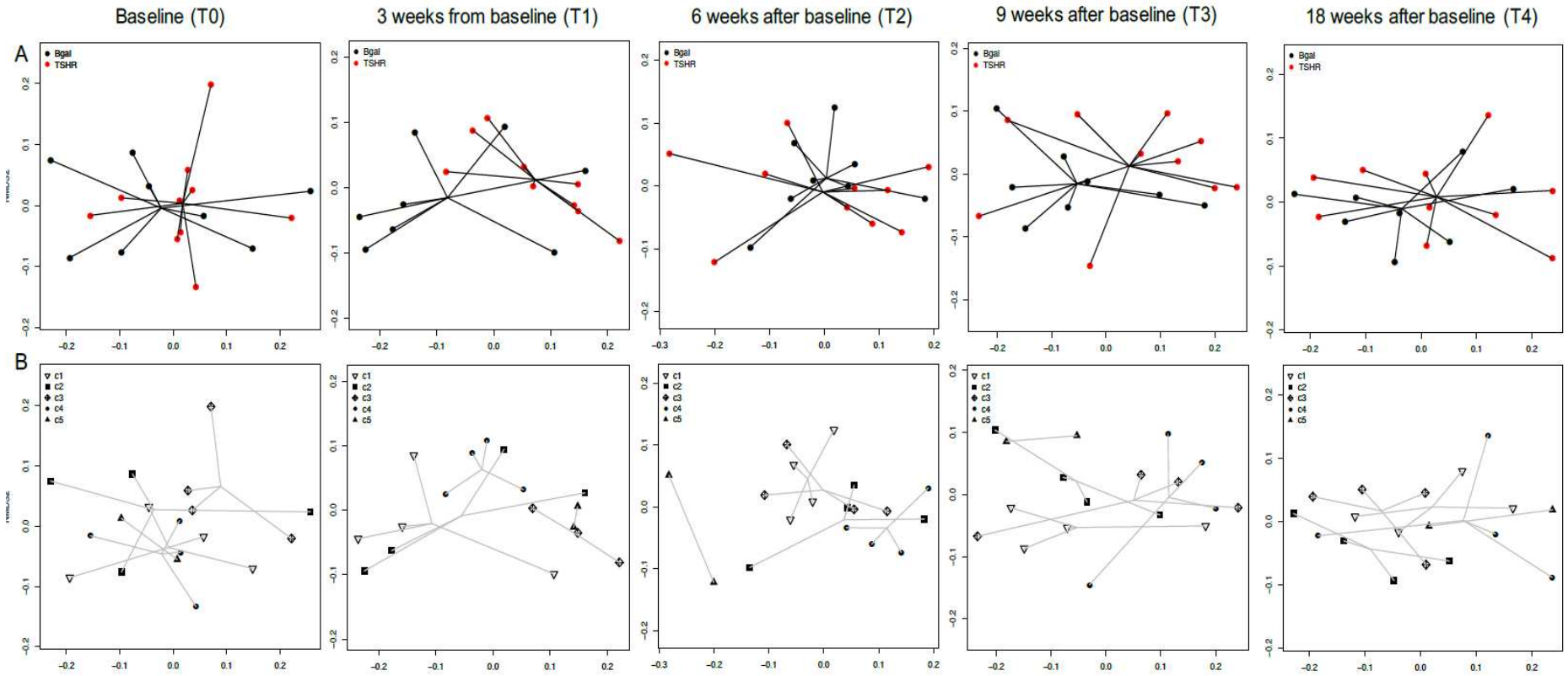

Additional file 6: Figure S1

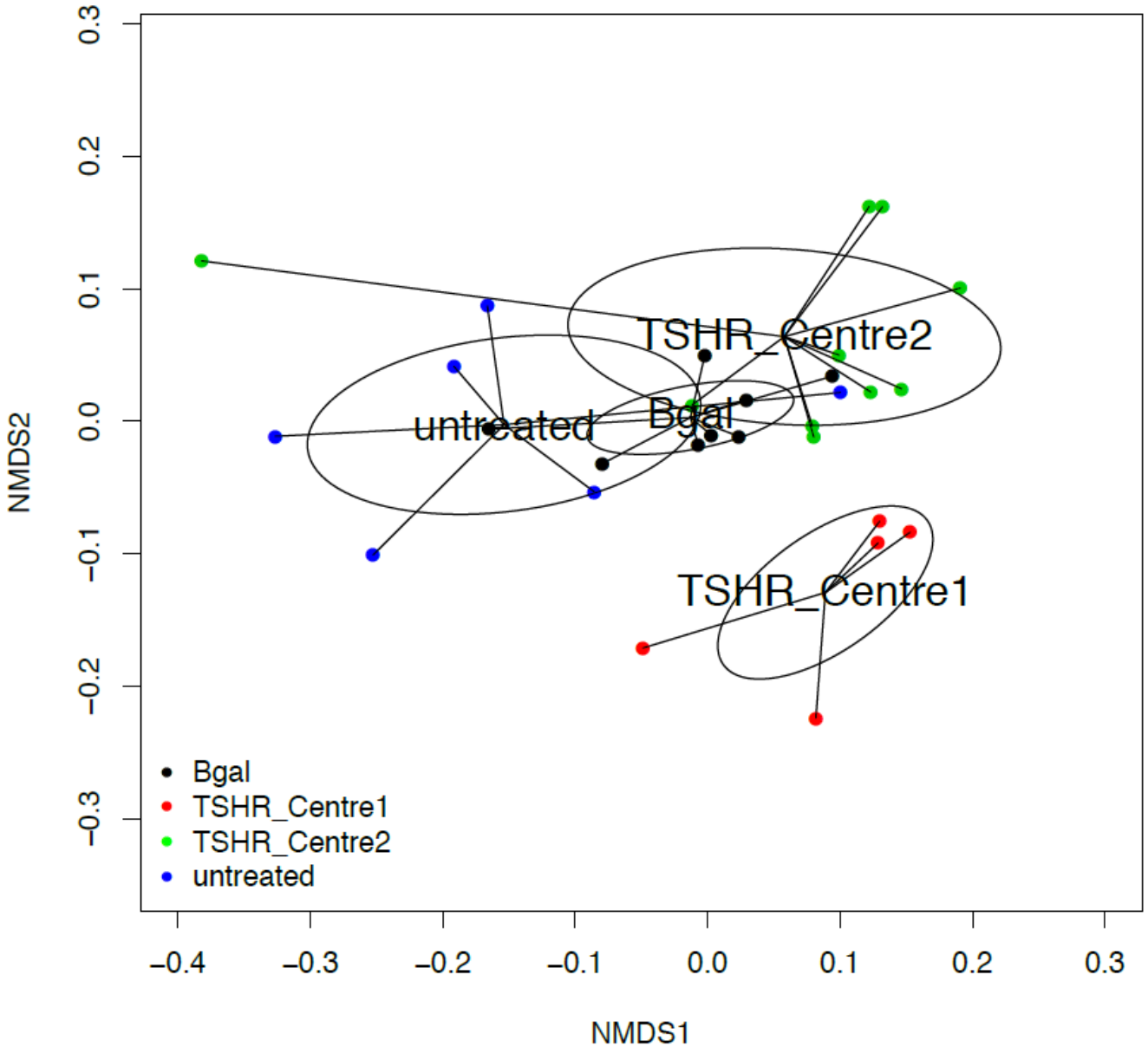

Additional file 7: Figure S1

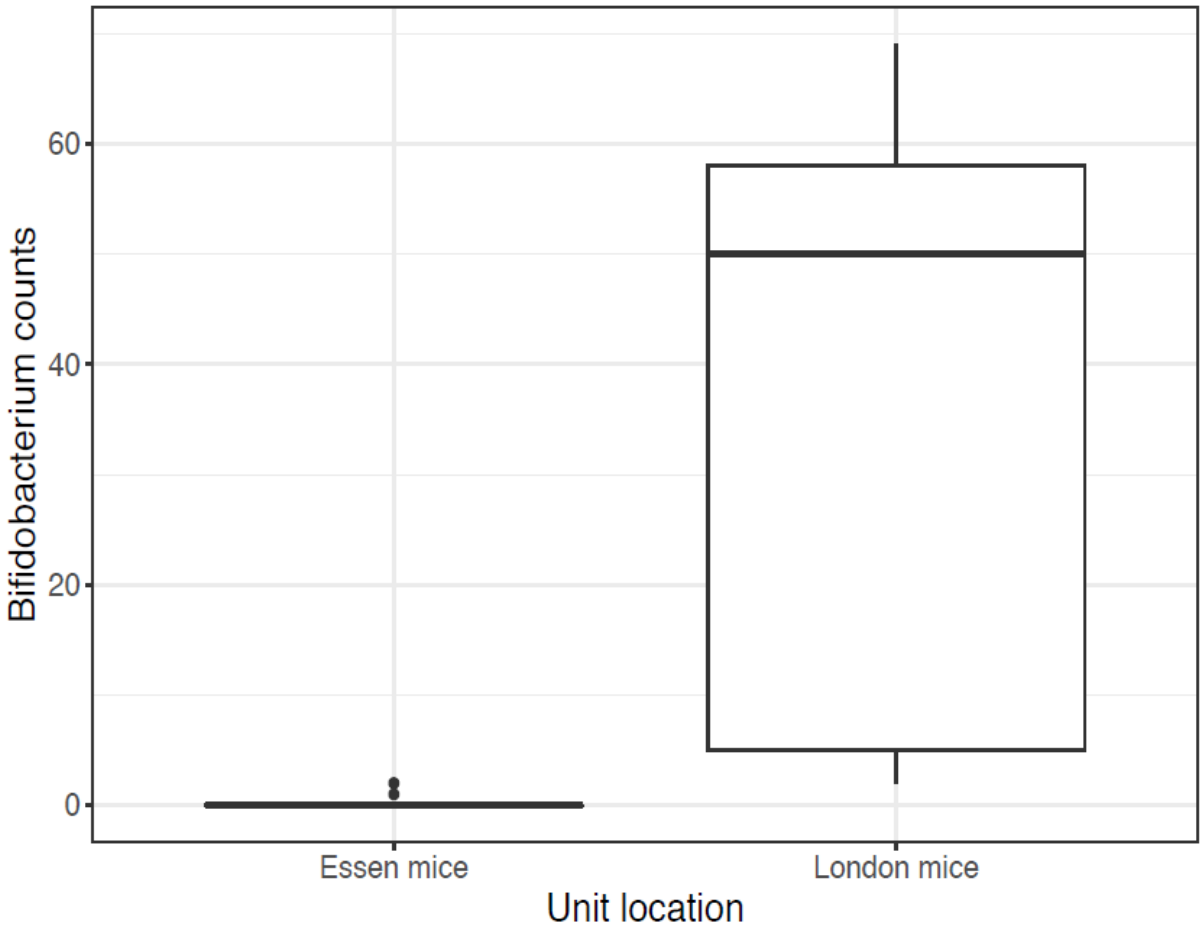

Fig 1

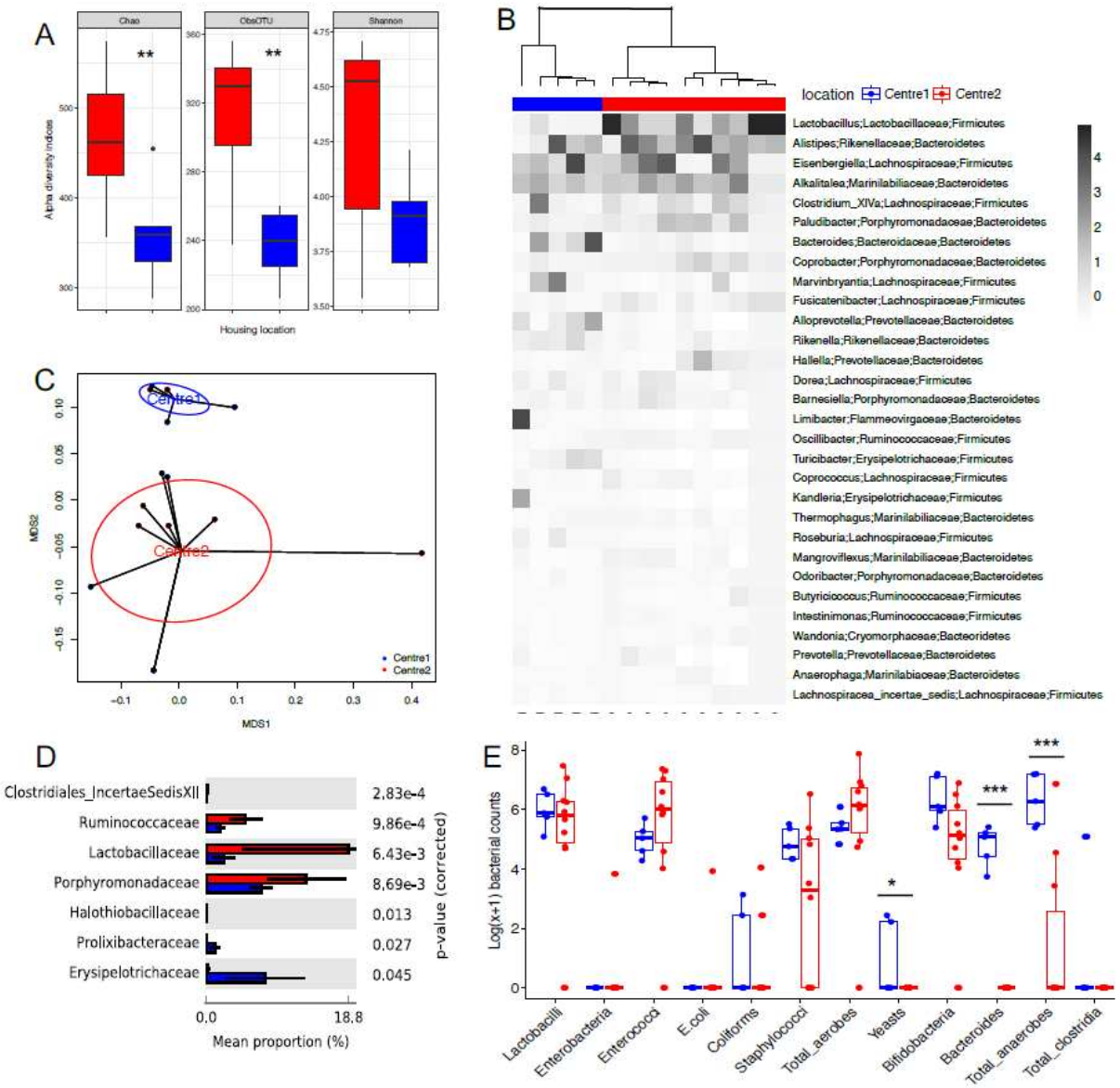
A
Chao
ObsOTU
Shannon
**
**
Alpha diversity indices
Housing location
B
location Centre1 Centre2
Lactobacillus;Lactobacillaceae;Firmicutes
Alistipes;Rikenellaceae;Bacteroidetes
Eisenbergiella;Lachnospiraceae;Firmicutes
Alkalitalea;Marinilabiliaceae;Bacteroidetes
Clostridium_XlVa;Lachnospiraceae;Firmicutes
Paludibacter;Porphyromonadaceae;Bacteroidetes
Bacteroides;Bacteroidaceae;Bacteroidetes
Coprobacter;Porphyromonadaceae;Bacteroidetes
Marvinbryantia;Lachnospiraceae;Firmicutes
Fusicatenibacter;Lachnospiraceae;Firmicutes
Alloprevotella;Prevotellaceae;Bacteroidetes
Rikenella;Rikenellaceae;Bacteroidetes
Hallella;Prevotellaceae;Bacteroidetes
Dorea;Lachnospiraceae;Firmicutes
Barnesiella;Porphyromonadaceae;Bacteroidetes
Limibacter;Flammeovirgaceae;Bacteroidetes
Oscillibacter;Ruminococcaceae;Firmicutes
Turicibacter;Erysipelotrichaceae;Firmicutes
Coprococcus;Lachnospiraceae;Firmicutes
Kandleria;Erysipelotrichaceae;Firmicutes
Thermophagus;Marinilabiliaceae;Bacteroidetes
Roseburia;Lachnospiraceae;Firmicutes
Mangroviflexus;Marinilabiliaceae;Bacteroidetes
Odoribacter;Porphyromonadaceae;Bacteroidetes
Butyricicoccus;Ruminococcaceae;Firmicutes
Intestinimonas;Ruminococcaceae;Firmicutes
Wandonia;Cryomorphaceae;Bacteoridetes
Prevotella;Prevotellaceae;Bacteroidetes
Anaerophaga;Marinilabiaceae;Bacteroidetes
Lachnospiracea_incertae_sedis;Lachnospiraceae;Firmicutes
C
Centre1
Centre2
MDS2
MDS1
Centre1
Centre2
D
Clostridiales_IncertaeSedisXII
Ruminococcaceae
Lactobacillaceae
Porphyromonadaceae
Halothiobacillaceae
Prolixibacteraceae
Erysipelotrichaceae
2,83e-4
9,86e-4
6,43e-3
8,69e-3
0,013
0,027
0,045
p-value (corrected)
0,0
18,8
Mean proportion (%)
E
Log(x+1) bacterial counts
Lactobacilli
Enterobacteria
Enterococci
E.coli
Coliforms
Staphylococci
Total_aerobes
Yeasts
Bifidobacteria
Bacteroides
Total_anaerobes
Total_clostridia

Fig 2

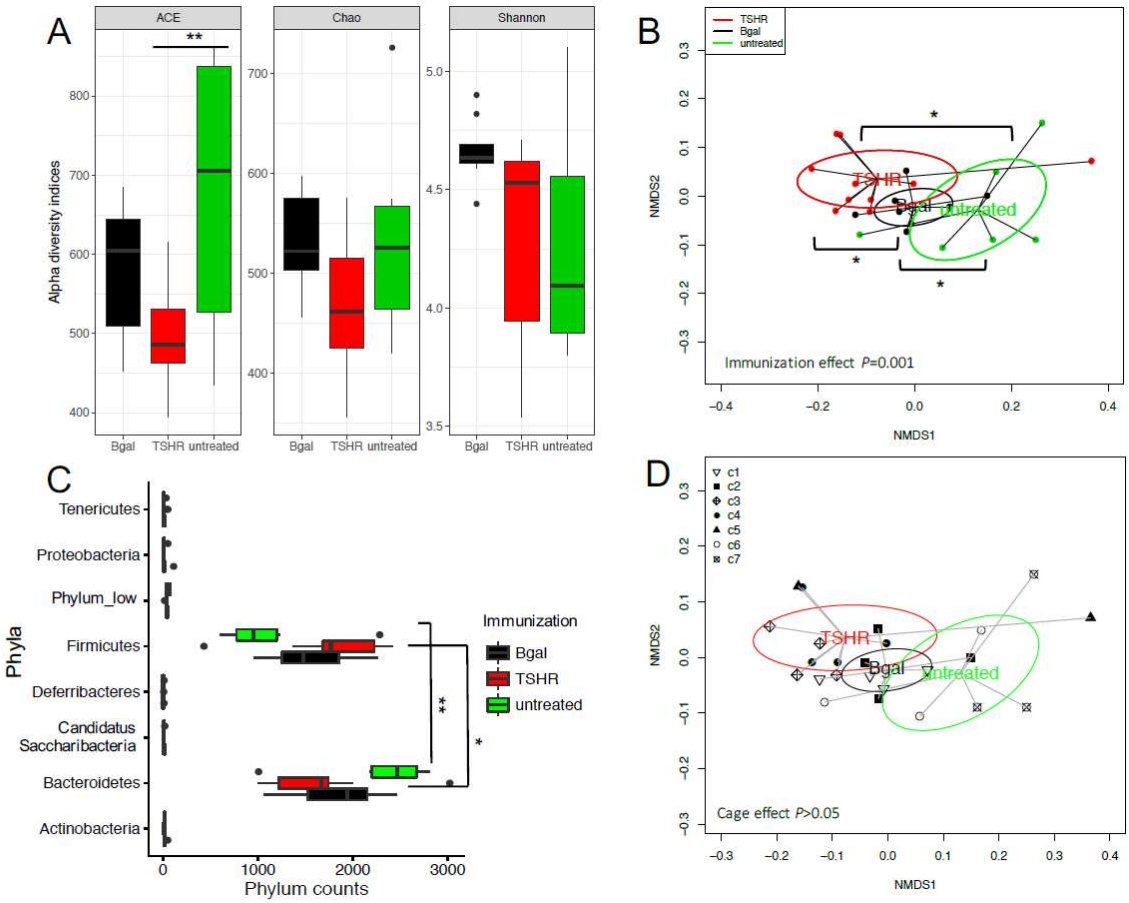
A
ACE
Chao
Shannon
Alpha diversity indices
Bgal
TSHR
untreated
B
TSHR
Bgal
untreated
NMDS1
NMDS2
Immunization effect P=0.001
C
Tenericutes
Proteobacteria
Phylum_low
Firmicutes
Deferribacteres
Candidatus Saccharibacteria
Bacteroidetes
Actinobacteria
Phyla
Phylum counts
Immunization
Bgal
TSHR
untreated
D
c1
c2
c3
c4
c5
c6
c7
Cage effect P>0.05

Fig 3

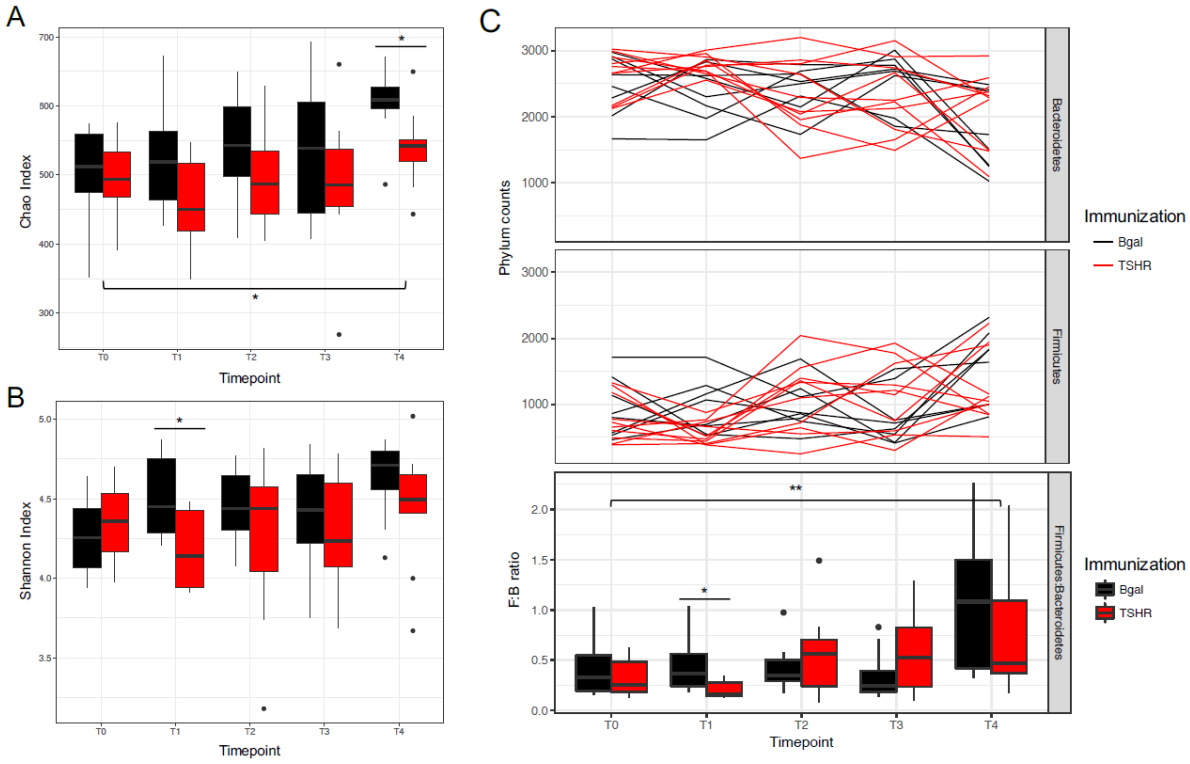
A
Chao Index
Timepoint
T0
T1
T2
T3
T4
B
Shannon Index
Timepoint
C
Phylum counts
Bacteroidetes
Firmicutes
F:B ratio
Firmicutes:Bacteroidetes
Timepoint
Immunization
Bgal
TSHR

Fig 4

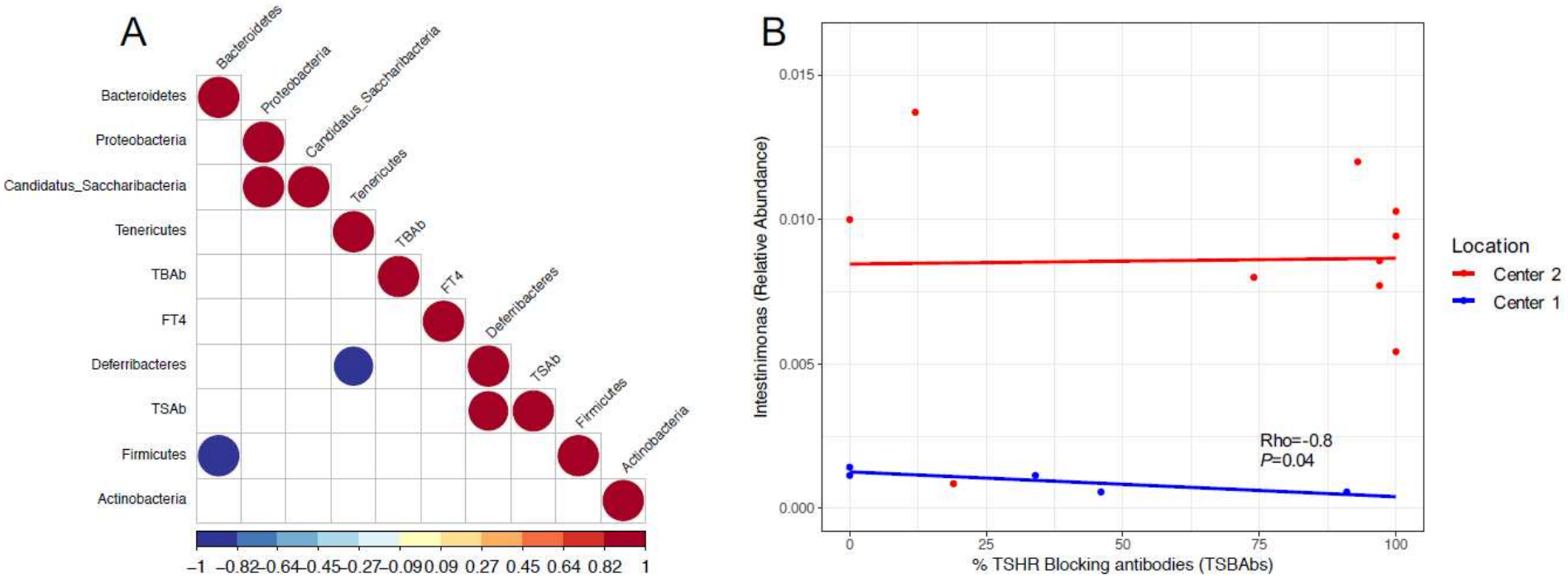
A
Bacteroidetes
Proteobacteria
Candidatus_Saccharibacteria
Tenericutes
TBAb
FT4
Deferribacteres
TSAb
Firmicutes
Actinobacteria
–1 –0.82 –0.64 –0.45 –0.27 –0.09 0.09 0.27 0.45 0.64 0.82 1
B
Intestinimonas (Relative Abundance)
0.015
0.010
0.005
0.000
0
25
50
75
100
% TSHR Blocking antibodies (TSBAbs)
Rho=-0.8
P=0.04
Location
Center 2
Center 1

Fig 5

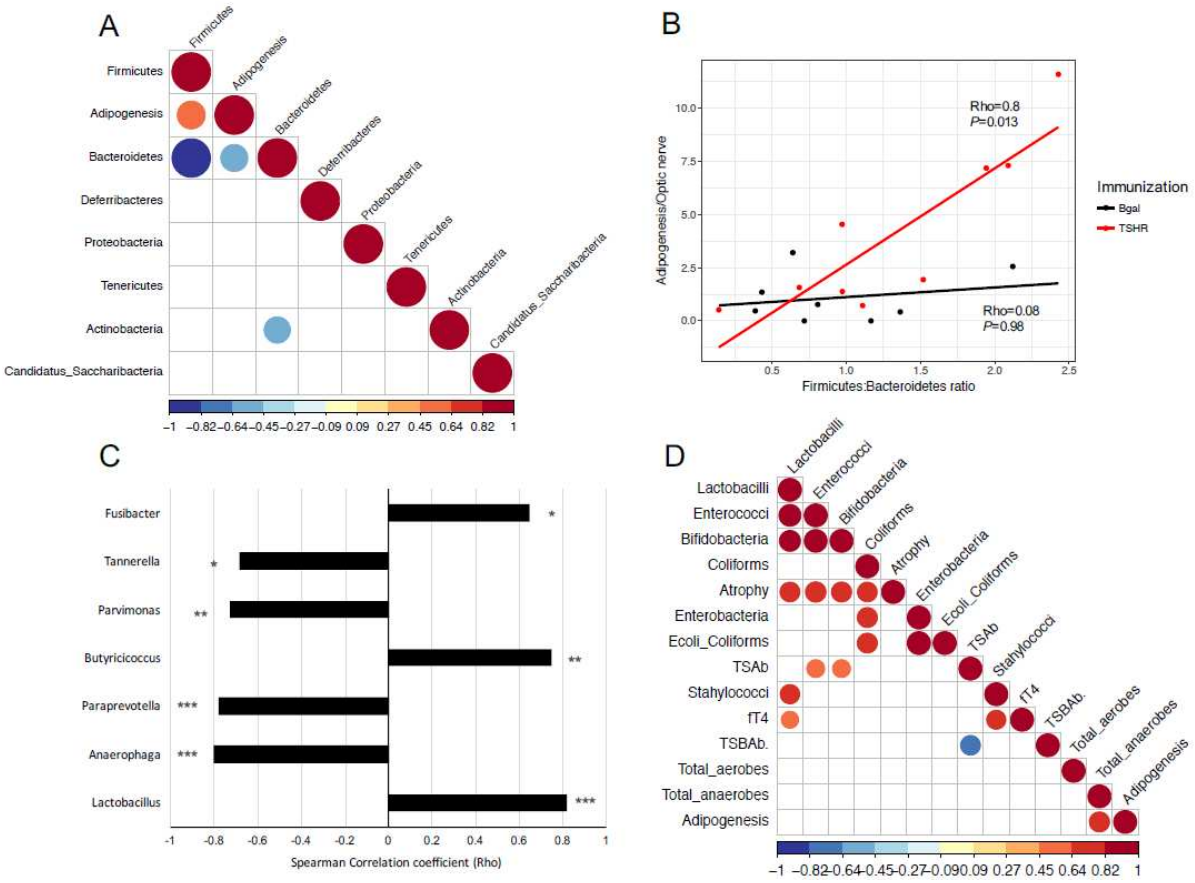
A
Firmicutes
Adipogenesis
Bacteroidetes
Deferribacteres
Proteobacteria
Tenericutes
Actinobacteria
Candidatus_Saccharibacteria
−1 −0.82 −0.64 −0.45 −0.27 −0.09 0.09 0.27 0.45 0.64 0.82 1
B
Rho=0.8
P=0.013
Rho=0.08
P=0.98
Adipogenesis/Optic nerve
Firmicutes:Bacteroidetes ratio
Immunization
Bgal
TSHR
C
Fusibacter
Tannerella
Parvimonas
Butyricicoccus
Paraprevotella
Anaerophaga
Lactobacillus
Spearman Correlation coefficient (Rho)
D
Lactobacilli
Enterococci
Bifidobacteria
Coliforms
Atrophy
Enterobacteria
Ecoli_Coliforms
TSAb
Stahylococci
fT4
TSBAb.
Total_aerobes
Total_anaerobes
Adipogenesis
−1 −0.82 −0.64 −0.45 −0.27 −0.09 0.09 0.27 0.45 0.64 0.82 1